

**LIBERATION AND CHARACTERISATION OF SOME NIGERIAN
MANGANESE ORES**

BY

UMELIWU, Onyeka Augustine

MEng/SIPET/2018/8737

**DEPARTMENT OF MECHANICAL ENGINEERING
FEDERAL UNIVERSITY OF TECHNOLOGY, MINNA,**

JANUARY, 2023

ABSTRACT

Nigeria is blessed with variety of solid mineral ores; manganese taking a good percentage. Nevertheless, no economic advantage has been derived because of

inadequate metallurgical processing. This work investigated the chemical, mineralogical characterization and measured the liberation of manganese ores from Ka’oje in Kebbi State, Madaka in Niger State, and Akampa in Cross River State, Nigeria. Three ore sample of manganese weighing 9.8kg, 46kg and 27.2kg was collected commuted and screened to varying sizes. The sample for the SEM were carbon coated and focus in the machine generating images at different magnification. The Scan Electron Microscope (SEM) was used to assess the morphology of the ores while the X-ray fluorescence (XRF) Spectrometer identified the compositions of the ore, X-ray diffraction (XRD) Spectrometer assessed the mineralogical phases present in the ore. The SEM in conjunction with the XRD disclosed the ores to be chiefly Spessartite with Ilmenite, Quartz, Albite and Chlorite as the major mineral in sample A and B, while Quartz, Ilmenite, Magnetite and Garnet in sample C. the XRF disclosed that the major elements present are Al, Si, Mn, Fe (mean value of 26.75%, 40.89%, 24.72%, 4.07% respectively), Al, Si, Mn, Ca, Fe (mean value 23.86%, 33.01%, 34.37%, 3.83%, 3.39% respectively), Al, Si, Fe (mean value of 31.2%, 41.6%, 15.6%, 8.67% respectively) for Sample A, B and C respectively. The particle size analysis showed liberation being attained for particle size below 75 μ m across the three samples. The work index was calculated to be 4. 3 kwh/ton, 2. 4 kwh/ton, and 2. 0 kwh/ton respectively. The data garnered from the characterization indicated the three samples to be low grade manganese ores and would enable identification of effective treatment method for better exploration of the ore deposits.

TABLE OF CONTENT

Title	Page
Cover Page	

Title	i
Declaration	ii
Certification	iii
Dedication	iv
Acknowledgement	v
Abstract	vi
Table of Content	vii
List of Tables	xi
List of Figures	xii
List of Plates	xv
CHAPTER ONE	
1.0 INTRODUCTION	1
1.1 Background to the Study	1
1.2 Statement of the Research Problem	2
1.3 Aim and Objectives	2
1.4 Justification	2
1.5 Scope of Research	3
CHAPTER TWO	
2.0 LITERATURE REVIEW	4
2.1 Minerals	4
2.2 Manganese Mineral	5
2.3 Operations in Mineral Processing	10
2.3.1 Liberation	10
2.3.2 Crushing	11
2.3.2.1 Types of Crushers	11

2.3.2.2	Jaw Crushers	11
2.3.2.3	Gyrator Crusher	12
2.3.2.4	Cone Crushers	13
2.3.2.5	Impact Crusher	14
2.3.3	Grinding	15
2.3.3.1	Ball Mill	15
2.3.3.2	Rod Mill	16
2.3.3.3	Autogenous and Semi Autogenous Mill	16
2.4	Theories of Comminution	17
2.4.1	Von Rittinger's Theory	17
2.4.2	Kick's Theory	17
2.4.3	Bond's Theory of Grindability	17
2.4.4	Berry and Bruce Theory	18
2.5	Liberation Analysis of Mesh Size	18
2.5.1	Shape Factor	19
2.5.2	Distribution of Particle Size	19
2.6	Liberation Processes	19
2.6.1	Sampling	19
2.6.2	Metallurgical Analysis	20
2.6.2.1	X-ray Diffraction	21
2.6.2.2	X-ray Fluorescence (XRF)	22
2.6.2.3	Scanning Electron Microscopy (SEM)	23
2.6.2.4	Sieve Analysis	24
2.6.3	Work Index	24
2.7	Modelling Mineral Liberation	25

2.8	Summary of Related Literature	27
2.9	Research Gap	28
CHAPTER THREE		
3.0	MATERIAL AND METHOD	29
3.1	Materials	29
3.2	Methodology	29
3.2.1	Preparation of Sample	29
3.2.2	Mineralogical Characterization	30
3.2.2.1	Scanning Electron Microscopy (SEM)	30
3.2.2.2	X-ray Diffraction (XRD) Spectroscopy	30
3.2.3	Elemental Characterization	31
3.2.3.1	X-ray Fluorescence (XRF) Spectroscopy	31
3.2.4	Sieve Analysis	31
3.2.4.1	Liberation Size Analysis	32
3.2.4.2	Work Index	32
3.2.5.	Physical Characterization	33
3.2.5.1	Density Determination	33
3.2.5.2	Hand Specimen Analysis	34
CHAPTER FOUR		
4.0	RESULTS AND DISCUSSION	35
4.1	SEM Analysis	35
4.2	X-ray Diffraction (XRD) Spectroscopy	36
4.3	X-ray Fluorescence (XRF) Spectroscopy	40
4.4	Sieve Analysis	46
4.5	Mineral Liberation	50

4.6	Work Index Calculations	51
4.7	Physical Analysis	62
4.7.1	Hand Specimen	62
4.7.2	Density determination	62
CHAPTER FIVE		
5.0	CONCLUSION AND RECOMMENDATION	64
5.1	Conclusion	65
5.2	Recommendation	65
5.3	Contribution to Knowledge	65
REFERENCES		66
APPENDICES		69

LIST OF TABLES

Table		Page
2.1	Manganese Minerals, Chemical Formula and Content	8
2.2	Properties of Manganese	9
4.1	Sample A XRF result showing constituent elements	41
4.2	Sample B XRF result showing constituent elements	43
4.3	Sample C XRF result showing constituent elements	45
4.4	Results for sieve analysis	48
4.5a	Sieve Size of particle (reference ore) feed to ball mill	52
4.5b	Reference ore particle size discharged from the ball mill	53

4.6a	Sieve Size of particle (Test ore Sample A) feed to ball mill	54
4.6b	Test ore particle size discharged from the ball mill sample A	55
4.7a	Sieve Size of particle (Test ore Sample B) feed to ball mill	57
4.7b	Test ore particle size discharged from the ball mill B	58
4.8a	Sieve Size of particle (Test ore Sample C) feed to ball mill	59
4.8b	Test ore particle size discharged from the ball mill sample C	60

LIST OF FIGURES

Figure		Page
2.1	Geological map of Nigeria showing occurrences of Manganese deposits	5
2.2	Working principle of a Jaw crusher	12
2.3	Working Principle of a Gyratory crusher	13
2.4	Working Principle of a cone Crusher	14
2.5	Working Principle of an Impact Crusher	15
4.1	Sample A XRD result, showing the various diffraction Peaks of the ore minerals	37
4.2	Pie Chart showing the phase percentage in Sample A	37

4.3	Sample B XRD result, showing the various diffraction peaks of the ore minerals	38
4.4	Pie Chart showing the phase percentage in Sample B	39
4.5	Sample C XRD result, showing the various diffraction peaks of the ore minerals	39
4.6	Pie Chart showing the phase percentage in Sample C	40
4.7	Variation of the element constituent Sample A	42
4.8	Variation of the element constituent of Sample B	44
4.9	Variation of the element constituent of Sample C	46
4.10	Variation of sieve analysis	47
4.11	Liberation Assay of Manganese Sample A-C	50
4.12a	Variation of sieve size against cumulative passing and cumulative retained of granite reference ore	52
4.12b	Variation of sieve size against cumulative passing and cumulative retained of granite (reference ore) product from ball mill	53
4.13a	Variation of sieve size against cumulative passing and cumulative retained of Manganese ore sample A feed to ball mill	54
4.13b	Variation of sieve size against cumulative passing and cumulative retained of Manganese ore sample A product from ball mill	55
4.14a	Variation of sieve size against cumulative passing and cumulative retained of Manganese ore sample B feed to ball mill	57

4.14b	Variation of sieve size against cumulative passing and cumulative retained of Manganese ore sample B product from ball mill	58
4.15a	Variation of sieve size against cumulative passing and cumulative retained of Manganese ore sample C feed to ball mill	60
4.15b	Variation of sieve size against cumulative passing and cumulative retained of manganese ore sample C product from ball mill	61
4.16	Variation of the density of the three samples	62

LIST OF PLATES

Plates		Pages
I	Ka'oje Manganese Ore Sample A	6
II	XRD, SEM and Electronic Weigh Machine	29
III	Three sieve sizes of manganese samples	31
IV	A-C SEM Images	35

CHAPTER ONE

1.0 INTRODUCTION

1.1 Background of Study

Mineral processing involves two major stages of comminution and concentration of the ores. Comminution involved reduction of the ore size into fragments that can be liberated from the gangue accompanied and subsequently allow for concentration of the ore. Concentration of ore is simply an act of separation. The degree of liberation is often determined by the type of separation process to be adopted for the ore treatment. It is important that the right degree of liberation be ascertained before comminution and concentration is begun, as comminution consumes quite enormous an amount of energy, it is therefore paramount to have that in mind before embarking on the process.

Liberation of valuable minerals from gangue at the coarsest of particle size is one of the objectives of comminution in processing of minerals (Wills and Napier-Munn, 2011).

Texture is the primary characteristics of ore liberation, on the locking of minerals with

gangue and grinding (Zang et al., 2013). An effective comminution hinges on the liberation. The liberation data can be garnered by mineralogical analysis processes using Scanning Electron Microscope (SEM) attached with an Energy Dispersive X-ray Spectroscopy (EDS), then predicting liberation by models (Donskoi et al., 2008 and Hamid et al., 2019).

1.2 Statement of the Research Problem

The manganese demand is highly concentrated but large quantity of manganese used in Nigeria is imported due to the exploration of ore deposit across the nation.

Ore deposits found in different location may have different characterisation and treatment method, such data are not readily available. The need to make this data available for effective beneficiation is appropriate to metallurgist and manufacturing industries.

The degree of liberation of three Manganese ore for effective value addition into a metallurgical grade is also not available. Thus, the need for this investigation.

1.3 Aim and Objectives

The aim of this work is to characterize and measure the degree of liberation of Manganese ores from three different locations in Nigeria.

This aim would be attained via the below objectives;

1. To characterize the manganese ore from the three deposits
2. To measure the degree of liberation and collect the data.
3. To calculated the work index needed in grinding the ore
4. To achieve the physical characteristics of the ores

1.4 Justification

The exploration of manganese would be better achieved if adequate analysis and data of the liberation process is known. It therefore, shows the best way of separating valuables and quantity obtainable and by extension, foster the steel production and rebuilding of steel plants for optimum utilization and development of local manganese production.

The manganese ore deposit in the three locations has the prospect to improve the needs for steel development in Nigeria. It has to be characterized, liberated and beneficiated to a metallurgical grade, however, the analysis of the liberation process is essential if this goal must be met.

1.5 Scope of the Research

This research work is based on the liberation and characterisation of Nigerian manganese ores, it intends to make data available as regards these ores and is only limited to three deposit located at Kebbi, Niger and Cross-River state only. These deposits would be subjected to the following analysis

- a. Scanning Electron Microscopy (SEM)
- b. X-ray diffraction (XRD) Spectroscopy
- c. X-ray Fluorescence (XRF) Spectroscopy

CHAPTER TWO

2.0 LITERATURE REVIEW

2.1 Minerals

Minerals are best described as substances that occur naturally, having specified chemical composition, crystal structure and physical characteristics (Halder 2018, Hassan 2013, Jones 2000). Although, not all materials classified as minerals are material with inorganic source or having a well-defined chemical composition and atomic structure. Therefore, it is easier to define minerals as substances that are rooted out from the earth having economic value (Wills and Munn, 2006). The major sources of minerals are the earth and recycled scrap.

Mineral processing is simply the separation of valuable mineral from the gangue. This is often achieved through exploitation of the distinction that exist in physical and chemical characterisation of the minerals (Wills 2015, Swapan 2018). This process could be achieved through physical means to produce an enrich portion. The process is often a trade-off between advancement in metallurgical efficiency and cost of milling, especially ores of low value (Wills and Munn, 2006).

The quest for the economic diversification in Nigeria can be achieved through exploration and value addition of the solid mineral to industrial standard. Nigeria is blessed with variety of solid mineral ores; manganese taking a good percentage. Nevertheless, no economic advantage has been derived because of inadequate metallurgical processing (Oyelola, 2020).

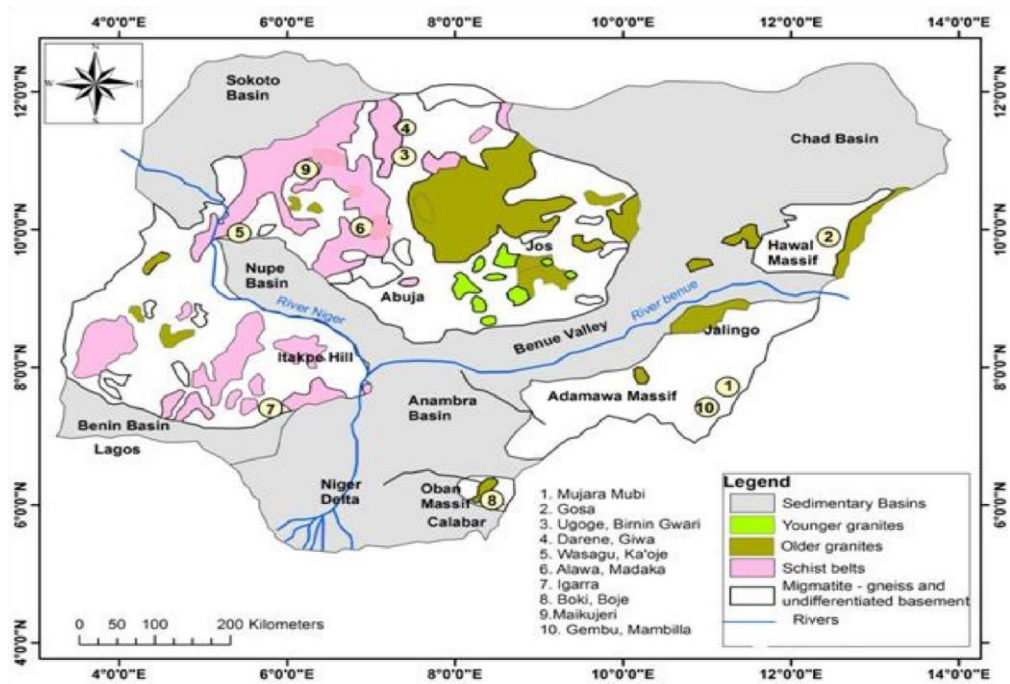


Figure 2.1: Geological map of Nigeria showing occurrences of manganese deposits. (Source: Akintola, 2019.)

The Figure 2.1 shows a geological map showing locations of manganese occurrence in Nigeria basins for possible exploration and value addition to the ores.

2.2 Manganese Mineral

Manganese is twelfth on the scale of the most abundant element on earth comprising about 0.1% of earth crust and its occurrence is primarily as pyrolusite (MnO_2), psilomelane $(Ba, H_2O)_2MnO_{10}$ and branunite $(Mn^{2+}Mn^{3+}_6)(SiO_{12})$. Pyrolusite being the most relevant. Manganese, a silvery grey substance that mask iron. It easily oxidizes, hardly fuses, brittle and hard in nature. It has a specific gravity of the range 7.13 to 8, boiling and melting point of $1900^\circ C$ and $123^\circ C$ respectively, its atomic weight is 54.6, manganese, obtained majorly from pyrolusite (manganese ore), often exist in combination with iron (Hassan, 2013).

Carl Wilhelm Scheele a Swedish chemist was the first in 1774 to discover new element, manganese. Gottlieb Gahn in continuance of his work isolated the impure chemical of manganese using carbon as the reductant.

Manganese was perceived to initially be the constituent that gave credence to Spartan's weaponry as superior. This gave room to finding that manganese increases hardness when added to iron without increase in brittleness (Alessio *et al.*, 2007, Tangstad 2013). Evolution of manganese in steelmaking saw light in the 19th century leading to more research and patents. The demand for Manganese is more in the steel industry especially, in ferroalloys. Although it has found use in making batteries (Muriana, *et al.*, 2014, Welham, 2002, Dell, 2000) and reagents. Manganese is also used as additives in deoxidation and desulphurisation in metallurgical industry, textile industries and in the manufacture of glass.



Plate I: Ka'oje manganese ore sample A

Manganese ores are classified according to their percentage of manganese constituent. Ores having percentage greater than 35 are classified as manganese ores; percentage range between 10 to 35, ferruginous manganese ores; while those between 5 to 10 known as manganiferrous manganese ores. Manganese could be divalent the most stable valency, trivalent or tetravalent in state, common among manganese minerals are oxides, sulphates and carbonates as listed in the Table 1 below.

Manganese, a greyish white metal has 25 as its atomic number on the periodic Table just between chromium-24 and iron-26. It also has an atomic weight of 54.9 and the most stable isotope of 55, it is hard and brittle in nature and it is categorized in the transition metal grouping. Its oxidation state ranges from 2, 3, 4, 6, 7 with a cubic, body centred crystal structure. Table 2.1 below shows some selected properties of manganese.

Table 2.1: Manganese Minerals, Chemical Formula and Content

Mineral	Chemical Formula	Manganese Content
Oxide Types		
Pyrolusite	MnO ₂	63.2
Vernadite	MnO ₂ .H ₂ O	44-52
Braunite	3(Mn,Fe) ₂ O ₃ .MnSiO ₃	48.9-56.1
Braunite II	7(Mn,Fe) ₂ O ₃ .CaSiO ₃	52.6
Manganite	γ -MnOOH	62.5
Psilomelane	(K,Ba)(Mn ²⁺ Mn ⁴⁺) ₈ O ₁₆ (OH) ₄	48.6-49.6
Cryptomelane	(K,Ba)Mn ₈ O ₁₆ .xH ₂ O	55.8-56.8
Hollandite	(Ba,K)Mn ₈ O ₁₆ .xH ₂ O	42.5
Todorokite	(Ca,Na,K) (Mn ²⁺ Mn ⁴⁺) ₆ O ₁₂ .xH ₂ O	49.4-52.2
Hausmannite	(Mn,Fe) ₃ O ₄	64.8
Jacobsite	Fe ₂ MnO ₄	23.8
Bixbyite	(Mn,Fe) ₂ O ₃	55.6
Manganocalcite	(Mn,Ca)CO ₃	<20-25
Oligonite	(Fe,Mn)CO ₃	23-32
Rhodochrosite	MnCO ₃	47.6
Rhodonite	MnSiO ₃	42
Tephroite	Mn ₂ SiO ₄	54.4
Alabandine	MnS	63.2
Gauerite	MnS ₂	46.2

Curled from Merete Tangstad book (2013); Handbook on Ferroalloys.

Table 2.2: Properties of Manganese

Property	Value
Atomic number	25
Atomic weight	54.938
Crystal structure	Cubic Body Centred
Valence states	2, 3, 4, 6, and 7
Melting point, °F	2275
Boiling point, °F	3742
Specific Gravity	7.21 to 7.44
Specific heat at 25.2°C, J/g	0.479
Density at Room Temperature, g/cm ³	7.21
Thermal expansion coefficient at 25°C, μm	21.8 x 10 ⁻⁶
Hardness, Mohr's	6
Latent heat of fusion, kJ/mol	12.91
Latent heat of vaporization, kJ/mol	221
Solubility	Soluble in water

Source: Manganese; Wikipedia (2021)

Manganese finds use in desulphurization and de-oxidation during steel making and production of Ferro alloys. Emphasis on the important of manganese is appreciated in the textile and ceramic industries, it also finds application in making of battery cells, dyes and paint and is key in the production of Aluminium alloy (Hassan, 2013).

2.3 Operations in Mineral Processing

Operations undergone during mineral processing can be classified into two major components; liberation and concentration (Wills and Munn, 2006).

2.3.1 Liberation

Liberation is the release of mineral valuables from the gangue contained in the ore. We liberate because the assemblage is intertwined with gangues, it is easily accomplished via comminution which is reducing the size of the ore by crushing and grinding to an extent of obtaining chiefly a clean mineral particle and gangue (Wills and Munn, 2006).

Grinding consumes more energy during comminution, estimably account for 50% of the total energy consumed during the concentration. The characteristics of feed ore during liberation is pivotal. When balance is sort, a finely grinded ore has a guarantee of recovering high number of valuables, but certainly not overgrinding to a fault of incurring loss in the finest fragments. It is therefore wise for metallurgist to seek optimization by controlling size reduction, liberation and size distributions since they are all interconnected.

The vantage of liberation is improving other operation of mineral processing. The product of comminution is usually exposed to enable classification in harmony to one or more properties such as magnetic separation, chemical affinity, density and size. Therefore, liberation analysis gives the pedestal to study behavioural distribution of particles and their classification.

2.3.2 Crushing

Crushing is the prior stage in comminution where the “run-of-mine” is fed into the crushing equipment to attain a reduction in size which can subsequently be useful for

liberation of the valuable from the intertwined gangue. It is often performed dry. The types of force are usually applied during size reduction. This may include; impact, compression and abrasion of which impact and compression are common as it relates to crushing. The gyratory, jaw and cone crushers are some of the equipment used in crushing.

2.3.2.1 Types of crusher:

Crushers are basically classified into two; Primary and Secondary crushers. Primary crushers are designed to collect large lumps from the mine and size them down after which the crushed or would be transferred for secondary crushing. Primary crushers are Jaw and gyratory crushers. While cone crusher is an example of a secondary crusher.

2.3.2.2 Jaw crushers:

The jaw crusher consists of two jaws acutely angled with one jaw fixed and the other able to swing relatively to the fixed jaw this can be explained as the mimicking of animal jaw movement. The ore is fed into the crusher from the top via a vibrating feeder or hopper. The jaws grip the ore and causes compression of the ores with the reduced sized ore allowed to drop downward into the discharge aperture (Haldar, 2018). The Figure 2.1 shows the pictorial view of the jaw crusher.

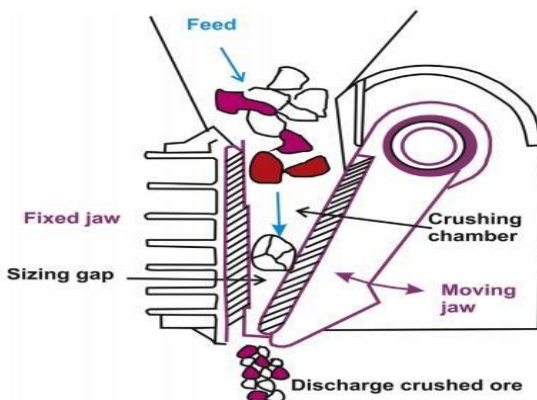


Figure 2.2: Working principle of a Jaw crusher

2.3.2.3 Gyrator crusher:

The gyratory crushers are surface lined with steel and have same operating concept as the jaw crushers. It has a conical chamber that allows for rotation in the path within the chamber and a head that holds the spindle which has an eccentric sleeve base and carries the grinding element (Haldar, 2018). As shown in Figure 2.3, the spindle can make turns along the eccentric sleeve axis which creates compression that crushes the ore lump between the rotary head and the top segmentation. It can take larger lumps due to the feed opening and has effective crushing ability (Wills and Munn, 2006).

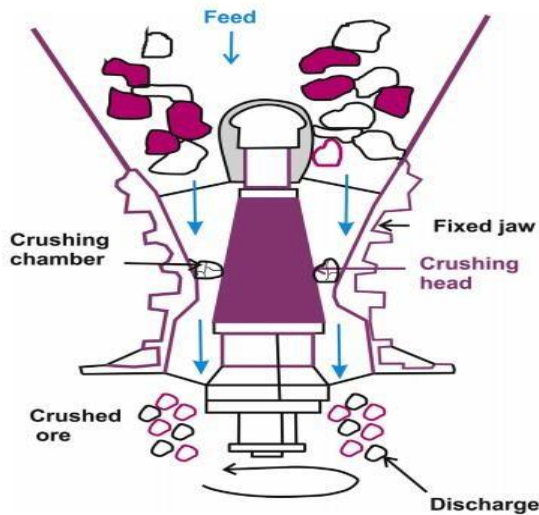


Figure 2.3: Working Principle of a Gyratory crusher

2.3.2.4 Cone crushers:

The crushing mechanism and design of a cone crusher is akin to the gyratory crusher, as shown in Figure 2.3, except for the fact that it has a spindle shorter which is supported at the base unlike the gyratory crushers whose spindle is suspended (Gupta & Yan 2006). The crushing chamber i.e. the mantle and concave are

also parallel and less slanted. These permits the production of fine particle owing to the prolonged retention of the ore particle. The breaking head is set into excitation inside an inverted cone. The crushing gap created during the opening and closing of the mantle and bowl liner induces a pressure for the crushing to take place. This opening and closing occur simultaneously both sides of the crushing chamber. The mantle head is responsible for steadying the head and is kept firm by collar bolted at the top by driving a nut through its thread region (Wills and Munn, 2006). Hydraulics are often used to hold firm the crushing shell which allows the passage of uncrushed ore (Gupta & Yan 2006).

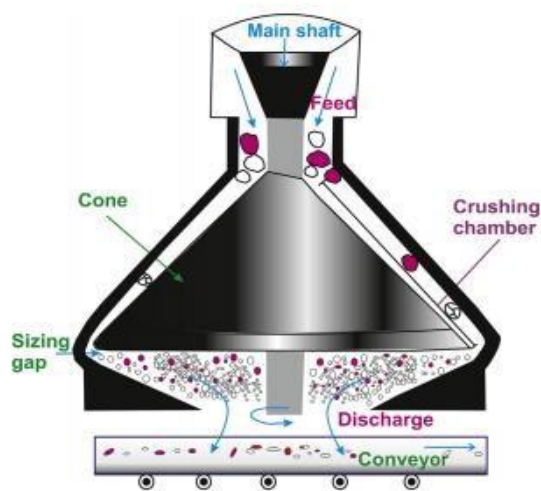


Figure 2.4: Working Principle of a cone Crusher

2.3.2.5 Impact crusher:

The impact crusher does not use compression pressure to crush materials rather, impact is utilized. The beaters of the crusher's transfers impact to the falling ores, which then smashes due to the build-up of internal stress resulting from the blow.

Crushing by impact and compression both have their advantages and disadvantages. For ores broken by compression, internal stresses still exist in the ore which can crack in

future; whereas that broken by impact would not because there is no residuum of stress in it. Figure 2.4 shows the working principle of an impact crusher.

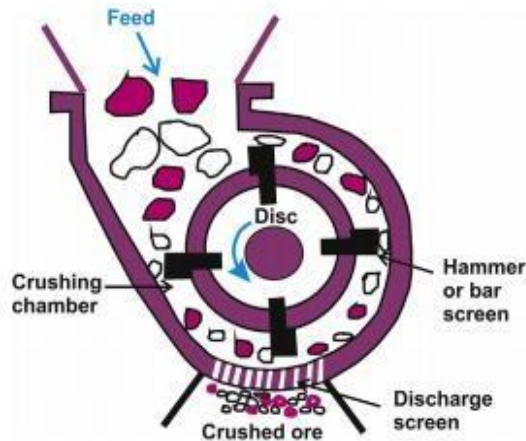


Figure 2.5: Working Principle of an Impact Crusher

2.3.3 Grinding

The grinding process often performed dry or suspended in water is targeted at the further reduction in size of ore particles using impact force. It is the final stage of comminution as it is usually executed in a vessel which is cylindrical and often in rotation.

The particles to be crushed are allowed to fall freely, which are met by the grinding medium, which administers force either by impact or compression, causing the comminution of the ore particulate. The grinding taking place in the mill could be influenced by the spacing of the grinding medium, the type of motion adopted, particle size and quality (Haldar, 2018).

The different types of grinding mills may include;

2.3.3.1 Ball mill:

This is made of a conical drum that rotates around its axis, the grinding medium are steel balls or cast iron which are agitated to rise and fall heavily on the material to be ground.

via the rotation of the drum. The operation of grinding on ball mills are done at increased speed to enable adequate striking of the materials by the balls. The ball mills produce a fine product given ample timing. There exist equal probability of the balls striking a fine or coarse particle (Duroudier, 2016).

For effective grinding to be achieved, the surface area of the balls is key. The smaller the balls the better, although the fed ore should be in classification of size such that it corresponds with the largest ball in the mill to exact just enough impact to cause disintegration of the ore (Wills and Munn, 2006).

2.3.3.2 Rod mill:

Rod mill has steel rods of at least 1.5 length to diameter ratio lined in a cylindrical or conical shell. The ratio is necessitated due to the need to avoid the tangling of the fed ore. The grinding is actualized by the contact made by the lined rods at covers the ends of the mills. The roll crushers are agitated into cohesion parallel to each other, such that particles would not be over grinded. The rod mill is operated at a lower speed when compared to the ball mill this is because the rods are rolled and not cascaded as in the ball mill (Duroudier, 2016), therefore need more attention and monitoring to avoid tangling of the rod due to misalignment which may further cause reduce the efficiency of grinding.

2.3.3.3 Autogenous and semi autogenous mill:

Autogenous mill is self- grinding and does not require another grinding medium. It uses large ore lumps to achieve comminution. The rotating drums sends into motion the particle to be crushed in cascading manner causing impact which result to size reduction. The semi- autogenous mill in it has small steel balls introduced into the equipment to assist in disintegration of the ores. This mill has found relevance because of the cheap

grinding medium which has replaced the need for rods and steel balls. Although the lumps introduced into the equipment should be to withstand impact for a longer time without breaking easily.

2.4 Theories of Comminution

2.4.1 Von Rittinger's theory:

Rittinger's imperative was that there is a proportionality between the energy consumed during size reduction and the new surface area formed. In other words, the surface area is inversely proportional to the diameter for a uniform weighed ore. This theory is expressed mathematically as (Wills and Munn, 2006);

$$E = K \left(\frac{1}{D_2} - \frac{1}{D_1} \right) \quad (1)$$

Where, E represents the Energy fed, D_1 and D_2 is the initial and Final size diameter and K, a constant.

2.4.2 Kick's theory:

Kick asserted that a proportionality exists between works required to decrease in volume of the particles of interest. It is stated mathematically as thus (Will's and Munn, 2016);

$$R = \frac{f}{P} \quad (2)$$

Where f is the diameter of particles feed, P is the product particle diameter.

2.4.3 Bond's theory of grindability:

Bond's (1996) theory conveys that the input from work has proportionality to the new crack tip length resulting from the breakage of the particle expressed as the difference in work from product and feed.

This is expressed mathematically as

$$W = 10W_i \left[\frac{1}{\sqrt{P}} - \frac{1}{\sqrt{F}} \right] \quad (3)$$

W represents the inputted work kilowatt hour; W_i is the work index in kilowatt hour.

2.4.4 Berry and Bruce theory:

Berry and Bruce (1966) came up with their own development which centred on the grindability of an ore sample, only that theirs was referenced to an ore of a known work index, whose power consumption is known from the time of grinding. The power consumed by the test sample is also gotten through the same process as the referenced ore of the same weight. Bonds equation can then be used to analyse, given that the referenced ore is represented by r and the test ore by t.

This process can give a viable result if both samples are pulverized to almost similar size distribution.

$$Wr = Wt = 10Wr \left[\frac{1}{\sqrt{P_r}} - \frac{1}{\sqrt{F_r}} \right] = 10Wt \left[\frac{1}{\sqrt{P_t}} - \frac{1}{\sqrt{F_t}} \right] \quad (4)$$

Therefore,

$$W_r = W_t = \frac{10W_r \left[\frac{1}{\sqrt{P_r}} - \frac{1}{\sqrt{F_r}} \right]}{10W_t \left[\frac{1}{\sqrt{P_t}} - \frac{1}{\sqrt{F_t}} \right]} \quad (5)$$

2.5 Liberation Analysis of Mesh Size

The role of some parameters in modelling cannot be emphasized. Factors like shape, initial ore texture and particle size distribution. These factors are usually accounted for

satisfactory modelling when the numerical model equals the real crushed sample characterized with these parameters in mind (Rozenbaum *et al.*, 2015).

2.5.1 Shape factor:

The least mesh of the sieve defined by letter d that allows the passage of sample fragment. The shape factor f defined as the ratio of the volume of the particle to the least mesh, measures the cubic shape deviation. I.e. the closest shape of the particle fragment is a sphere and the shape factor differs with minerals of varying sizes (Rozenbaum *et al.*, 2015).

2.5.2 Distribution of particle size:

Experimental data of the measure of the distribution of the practical size can be regulated to fit analysis, which may require development of curves through mathematical syntax and regulate the necessary parameters to suit that of the experimental, although the setup should allow easier calculations of the analytical to the experiment. Rosin-Rammler model could be considered valuable model (Rozenbaum *et al.*, 2015), there, the distribution of particle size was illustrated as $g = d_{95}/d_5 > 4$ for quite a number of ore samples.

2.6 Liberation Processes

Liberation processes are often employed during mineral beneficiation, and these processes are stepwise as thus;

2.6.1 Sampling

A sample is a specimen that represent part or a single object from a bulk or group mainly for analytical purposes. The goal of sampling in mineral processing is recovering a speck

from the bulk ore to represent the larger batch and subject it to laboratory analysis, the value of the sample is dependent on the volume of the samples represented and care should be taken to ensure adequate and sure-enough representation. It is of importance to the best possible that samples be collected when reduction towards sizing to smaller particles have already been accomplished (Wills and Munn, 2006). Although there are salient reasons why metallurgist embark on sampling and may include;

1. Identification of the chemical composition of the specimen
2. To query the requirement, meet of the specimen
3. To organize other metallurgical analysis such as micrographic analysis
4. For metallurgical accounting purposes.
5. To make known the losses and recovery in order to minimize losses and maximize recovery.

Gy (1979) purported a formula to determine the sample size that best fits, that is closely considering the shape of the particle, the degree of liberation achieved and the particle size of the sample. Gy's formula when the minimum weight is considered smaller than the gross weight is expressed as

$$M = \frac{Cd^3}{S^2} \quad (6)$$

Where M is the minimum weight of sample required in grams, C represented the sample material constant in grams per cubic centimetre, d is the dimension of the largest piece of sampled in centimetre and s is the procedural error for balance in the process (Wills and Munn, 2006).

2.6.2 Metallurgical analysis

The determination of the chemical, mineralogical and compositional phases of material using conventional methods or using instruments is often prescribed as metallurgical analysis. The conventional methods use chemical reactions in the analytic process whereas the instrumental require application of certain instruments which may include; the X-ray Powder Diffractometer, Mineral Liberation Analyser (MLA), FTIR Spectrometer, High Temperature Furnaces, Qualitative Evaluation of Minerals by Scanning Electron Microscopy (QEMSCAN) amongst numerous, most often the instrumental values are compared with an already known standard as a reference.

2.6.2.1 X-ray diffraction (XRD):

X-ray diffraction is analytic in technique and have found use majorly in crystalline material for identification of phases, orientation of crystals and structures. It is non-destructive, although the analyzed material is often pulverized.

The cathode ray tube is the dispenser of the X-ray which is interfered by crystalline specimen (solid) and monochromatic X-ray, churning out monochromatic radiation which is focused and paralleled on the sample. This constructive interference from the monochromatic beaming angled at different dispersion on a lattice plane produces a peak, the intensity of the peak is used to ascertain the lattice distribution of the atom of the specimen. This condition satiates Bragg's law which is represented as (Wills and Munn, 2006):

$$n\lambda = 2d\sin\phi \quad (7)$$

Where n denotes integer; λ , Wavelength; d is the diffraction spacing and ϕ is the angle of diffraction. A very crucial component of the diffraction is the existing angle between the incident and diffracted rays.

Identification of minerals is reached when the diffracted peak is collected into inter planer d spacing and contrasted with an already standardized pattern of reference (Andrei *et al.*, 2015).

2.6.2.2 X-ray fluorescence (XRF):

The X-ray fluorescence spectrometer is an instrument used to measure the excitation of incident sample radiation. It is also nondestructive in analyzing characterisation of materials and probing the elemental and chemical constituent of minerals, Geological excavations, metals, glass and ceramics.

XRF comprise basically to components; the x-ray out and a detective sensor that detects the rays of fluorescence from light of incidence. When a beam of x-rays is cast upon the material, the electrons in the inner atoms becomes excited and subsequently displaced from orbits on the shell. The vacancies created are filled by atoms via dethronement of electrons from higher orbitals on the shell within or outside the atomic sphere, thereby causing a decrease in the binding energy of the higher shell orbits and is termed fluorescent radiation. Since the energy of the photon emitted is that of a transition between specified electrons shell in designated elements, the fluorescence rays produced can be used in detection of elemental abundance in samples, the wavelength of the fluorescent radiation well obeys Planck's rule (Karl *et al.*, 2011):

$$E = \frac{hc}{\lambda} \quad (8)$$

Where

λ = wavelength

E = Energy State difference ($E_1 -$

E_2) h = Planck's constant C =

Light Velocity.

The wavelength when properly separated during analysis determines the element present in the samples, whereas, the intensity of energy obtained by the detector's accounts for the abundance of element in the sample (Karl *et al.*, 2011).

2.6.2.3 Scanning electron microscopy (SEM):

Scanning Electron microscopy uses the scanning electron microscope to scan the surface of a sample with an array of electrons, thereby producing the image of the sample. There is an interaction between the sample atoms and signals topographic data of the sample surface and composition. SEM is non-destructive owing to the fact that there is no volume loss in the sample during the process, therefore cycle of experiment can be done on the same sample. The interaction between the electrons and the sample produces secondary electrons, characteristic X-ray, cathodoluminescence (visible light), reflected scattered electrons as signals which are picked by some detectors to produce images that are displayed on the screen. There is a depth of penetration resulting from the beam of the electron hitting the surface of the sample, this penetration could reach microns deep which is a function of the interplay of the accelerating voltage and the sample density. This interaction in the sample is the formative factor for most signals, while the secondary electrons find value in topographic and morphological imaging, the backscattered electron adumbrate compositional contrast a multiphasic sample.

The resolution that can be maximally obtained in SEM is dependent of quite a number of factors, the depth of interaction between the sample and the electron beamed the spot size of the electron (Swapp, 2017).

2.6.2.4 Sieve analysis:

Sieve or gradation analysis is the oldest method of determining the size distribution of mineral particles. It gives room for easy determination of liberation size and the level of associations accompanying the mineral. The experiment is conducted using standard sieves of various mesh size placed on a shaker in descending order, although hand sieves are not entirely ruled out as it has also found application. The sieves are perturbed to enable ample and equivalent exposure to sieve passage. Given ample time smaller sized particle would pass through the sieves. Nevertheless, the larger particle could exert undue stress on the apertures if prolong excitation is allowed. There is usually a constraint of near sized particle that becomes an obstruction to the free passage of particles causing blinding and by extension decreases the efficacy of the sieving apparatus. The blinding becomes of more concern with smaller aperture sieves (Wills and Munn, 2006). The result is often presented as percentage of the mass owing to the fact that the sample experimented upon are only representations of an entire lot. Sieve analysis can be done on a broad range of material ranging from sands, coals, inorganic and organic substances metals, grains and other materials.

2.6.3 Work index

Work index of an ore is crucial for effective design of mills where crushing and grinding would be done, it always comes handy in an attempt to reduce the size of an ore. The grindability of a material is known by the work index, that is to say the higher the work index value, the more the energy is required to crush the material or ore. The Bond work index has found a wider use in the test for grindability. It is simply the ease at which

reduction of ore is achieved and is defined as energy required to grind an ore from a batch size to passing 100 μ m sieve mesh (Hassan, 2013).

2.7 Modelling Mineral Liberation

Mineralogical analysis is often employed to obtain properties that related to the liberation of particles. These properties can be acquired by estimation, through the breakage of the particle and direct amassment of the liberation data informed through mineralogical analysis of sizes and classes of the samples. Crucial of such information would include; size distribution, chemical composition, classification of particles, density, porosity and mineralogy. This information can be acquired through XRD and XRF analysis, Pycnometry, chemical analysis, densification using heavy fluid, image and microscopic analysis and size analysis (Donskoi et al., 2008).

Guadin (1939), proposed that the mineral analysis of the texture of an ore is a good base for modelling liberation. This he simplified by as a function of the size characterize by the liberation particle size distribution, he assumed a cubed shaped grain and superimposed a fracturing system on the texture of the ore giving momentum for other research that follows.

Weigel (1975), proposed his own theory in furtherance to that proposed by Guadin, he considered the grain and size distribution. King (1979) contributed by probing the linearly a polished surface image and obtaining an intercept of the interested phase distribution. This corresponded to a non-preferential particle reduction in the size and class of study.

Gay (2004), Applied random breakage to the particle artificially to obtain an estimate of the sectional distribution of the particle, also he asserted that applying stereological correction gives better liberation properties, and advice that the distinction between linear intercept and particle section distribution should be used when estimating particle composition distribution as a source of guide.

King (2012), further developed a beta function for depicting approximately the distribution and shape of both the valuable and the gangue use α and β as the parameters, although it has found applicability with either a low- or high-grade ores content that enjoy varying mineral, this estimation can be actualized using the formula (Hamid et al., 2019).

$$P(g) = (1 - L_0 - L_1) g^{\alpha-1} (1 - g)^{\beta-1}$$

$$B(\alpha, \beta) \quad 0 < g < 1 \quad (9)$$

The average grade is represented as g , i.e. from random grinding of the host ore. α and β are the parameters whereas $B(\alpha, \beta)$ the function of distribution. (Hamid *et al.*, 2019) determined liberation model of scheelite ore, they used quantitative mineralogy in characterisation and simulated the model using MATLAB software by backward calculation, employing grade-size distribution by testing in batch concentration. The model gave a linkage to beta distribution function.

Weigel (2006) approached liberation distribution from the ore texture, he designed a linear programme to calculate using the balance total and component volume in conjunction with directional coefficient to ascertain the distribution provided that the product and initial feed contains the same mineral composition. Nonetheless, observation had it that more unknown directional coefficient seems to outnumber the linear equations used and that few numbers were actually needed to get the result. The equations he used was summed up as thus,

$$\sum_1 V(1, J) Q(1, 11, J) = (11, J + 1) \quad (10)$$

$$\sum_{11} Q(1, 11, J) = 1 \quad (11)$$

$$\sum_{11} Q(1, 11, J) MV(11) = MV(1) \quad (10)$$

Where;

$V(1, J)$ represent amount particle size J of composition 1

$Q(1, 11, J)$ represents the directional coefficient from composition $l - 11$

$MV(1)$, the mean value for composition 1

1, is the index of composition for initial particle size J

11, index of composition for the finer particle size $J+1$

2.8 Summary of Related Literature

Mariano (2016), Validated already done researches on ore textures and reached a conclusion that a liberation model in 3D gotten through X-ray tomography on random breakage of ore particles did not predict with precision the liberation distribution of the cross-sectional area and volumetric by impact breakage. She went further to advocate that there was no meaningful effect in a given size fraction in 2D measured using (metallurgical Liberation Analysis) MLA on the degree of liberation.

Yaro (2020), characterized Wasugu Manganese ore, which was Spessartite, with the average degree of liberation to be 50.14%.

Gbadamosi *et al.*, (2021) worked on the Petrological, Chemical, and Mineralogical Characterisation of Anka (Zamfara State) Manganese Ore. The manganese ore has a Spessartine phase and having 52.50% manganese. The author did not consider the energy needed to crush the ore, therefore the efficiency of exploring the deposit have not been completely ascertained. While Hassan *et al.*, (2013) also characterized and liberated Wasugu manganese ore.

Oyelola (2020) upgraded a low grade Wasugu-Danko manganese ore using gravity separation method. He characterized the ore using the XRD machine to be Spessartine and having a liberation size from the XRF analysis of 25.87% Mn

2.9 Research Gap

The review of literature has identified some essential gaps in existing knowledge

- The manganese ores from Akampa in cross river have not been researched on.
- Most researches done on ka'oje and Madaka deposit did not explicitly consider the work index and degree of liberation.

CHAPTER THREE

3.0 MATERIALS AND METHODS

3.1 Materials

Samples of Manganese ore from three different deposits (Ka'oje in Kebbi, Madaka in Niger, and Akampa in Cross River States of Nigeria) sample A, B and C were respectively used for the research work. The equipment used was a crusher, Standard sieve shakers, X-ray Refractory Spectrometer (XRF), X-ray Diffraction Spectrometer (XRD), Scan Electron Microscope (SEM), Electronic Weigh Balance and Measuring Cylinder.



Plate II: XRD, SEM and Electronic Weigh Machine

3.2 Methodology

The method used for the analysis, the selection of different sample sizes from the sieve analysis and sample preparation for different analysis is presented.

3.2.1 Preparation of sample

Three ore sample of manganese weighing 9.8kg, 46kg and 27.2kg was collected commuted and screened to size ranging from +20000 μm , -20000 + 14000 μm , -14000 + 10000 μm , -10000 + 6300 μm , -6300 + 5000 μm , -5000 + 3350 μm , -3350 + 2360 μm , 2360 +2000 μm , -2000 +1180 μm , -1180 + 850 μm , -850 + 600 μm , -600 + 425 μm , 425 + 300 μm , -300 + 150 μm , -150 + 75 μm , and -75 μm .

The preparation for the SEM was done as follows: the ore was carbon coated, placed on the sample holder at a located point. Sample port on the machine was now opened and the sample holder was carefully placed before the compartment was locked and the analysis was run. After some seconds a sound signifying a ready sample was heard. The focusing got done, then image generated by shifting to SEM mode and the display of generated image was automated at different magnification.

The preparation for XRD saw the mixture of the sample with a binder after which is was pelletized using a pelletizing machine at a high pressure, the sample was placed on a desiccator for analysis while the XRD machine was being warmed by turning it on.

Appropriate programs were engaged for elements of interest to analyze for their present in the ore.

3.2.2 Mineralogical characterisation

The mineralogical characterization was carried out using ISO 13322-1 :2004 particle size standards

3.2.2.1 Scanning electron microscopy (SEM): The morphology of the samples was investigated after polishing the surface and exposing to SEM.

3.2.2.2 X-ray diffraction (XRD) spectroscopy:

Quantitative analysis was carried out on the three samples of sieve size 75 μm using the XRD spectrometer to generated patterns and merging peaks to quantify the wealth of mineral present in the pulverized sample.

3.2.3 Elemental characterisation

3.2.3.1 X-ray fluorescence (XRF) spectroscopy:

Three different sieve sizes for the three samples were randomly selected for further assay of non-destructive XRF analysis geared towards ascertaining the elemental constituent of the samples and by extension determining the percentage manganese in the sieve size for each sample. The sieve sizes are -2000 +1180 μm , -6000 +425 μm , 75 μm . the investigation was done at National Steel Raw Material and Exploration Agency located in Kaduna.

3.2.4 Sieve analysis

Size analysis of the samples was carried out in order to determine the cumulative percentage retained and percentage passing out. The size on three different sieves for

each sample was analyzed further for the percentage of manganese content using XRF spectrometer. The ore samples were stacked with different mesh sieve sizes graduated in descending order, a duration of 20mins was chosen for the screening and the data collected was analyzed.



Plate III: Three sieve sizes of manganese samples

The calculations were as such,

$$\text{Percentage sample Retained} = \frac{\text{Weight Retained}}{\text{Total Weight}} \times 100 \quad (15)$$

$$\text{Cummulative Percentage Passing} = 100 -$$

$$(\text{Cummulative Percentage Retained}) \quad (16)$$

3.2.4.1 Liberation Size Analysis

The size at which the liberation of manganese is most optimal would be ascertained by passing each screen size retained to XRF spectrometry, to determine the percentage manganese present in the content of each particle size of the sample using the formula.

$$\text{Degree of Liberation} = \frac{\text{Total number of Free Particle}}{\text{Total Number of Free Particles+Locked Particles}} \times 100 \quad (17)$$

This is used to determine the extent of liberation of the valuables from gangue attained and forecast if upgrading of the ore would be possible by sizing and classification.

3.2.4.2 Work Index

The work index of the manganese ore was determined and the quantity of energy required to comminute. This would be determined using Bonds equation (Equation 5).

3.2.5 Physical Characterisation

The ore was analyzed to determine its physical properties which includes; the density of the ore, physical appearance and attraction to magnetic field. This analysis is vital to understanding what the content of the ore is before they are subjected to any other chemical analysis.

3.2.5.1 Density Determination:

The pycnometer (density bottle) was used to measure the specific gravity of the three ore (A, B, and C). The empty bottle was weighed and the recorded as W, afterward, the samples thrust into the pycnometer, weighed and recorded as W1. The pycnometer with the sample loaded in it is then filled with water, weighed and recorded as W2. Finally, the samples were removed and the bottle filled with water only was weighed and recorded as W3.

The density was then obtained using the formula

$$\text{Density} = \frac{\text{Sample Weight}}{\text{Sample Volume}} \quad (12)$$

Where, *Sample weight* = $(W1 - W)$ and

Sample Volume = *Mass of Water Displaced*

$$= (W3 - W) - (W2 - W1) \quad (13)$$

$$Density = \frac{(W1-W)}{(W3-W)-(W2-W1)} \times 100 \quad (14)$$

3.2.5.2 Hand specimen analysis

The sample was analyzed by hand for colour and magnetic properties by physically bringing a magnet close to the ore to see if an attraction would happen.

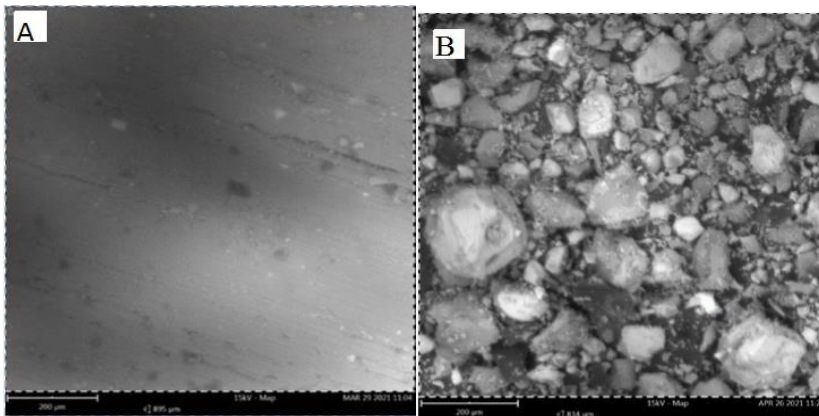
CHAPTER FOUR

4.0

RESULTS AND DISCUSSION

4.1 Scanning Electron Microscopy (SEM) Analysis

The SEM- Phenom pro X model machine with the following settings FOV: 895 μm , Mode: 15kV - Map, Detector: BSD, the pulverized sample of mesh size of 425microns form A, B, C was selected for SEM analysis for better understanding of the ore. The Figure 4.7 shows the SEM result for the three samples A, B, C respectively.



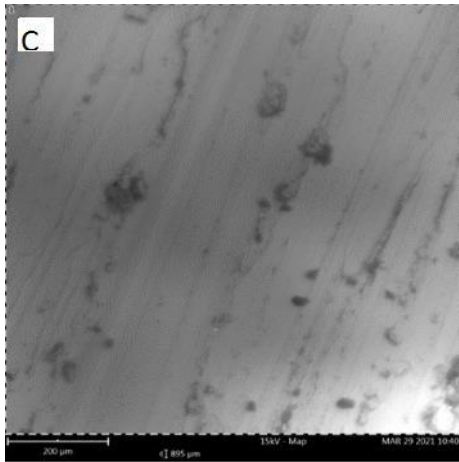


Plate IV: A-C, SEM image indicating Mn-rich region, Al and Si region and depicts complexity of the ore. FOV: 895 μm , Mode: 15kV - Map, Detector: BSD Full Three phases can be seen distinctly from the SEM result. First, the dark spot like zone, the white platy zone and the gray area. The dark spot shows the presence of rich Manganese and low iron whereas the white platy granules depicts the presence of high iron and low manganese as posited by Lingyun *et al.*, 2017, then the gray area shows high richness of silicon, aluminum with very negligible percentage of manganese. Confirming an intimate association of the ore with other minerals which cannot be physically separated except with the aid of other complex techniques (Yaro *et al.*, 2020)

4.2 X-ray Diffraction (XRD) Spectroscopy

Quantitative assessment of quantum presence of Mn and other constituent contained in an ore is pertinent for the grading of manganese ore, and the method of upgrade to be employed and even its applicability (Sajjad *et al.*, 2019). A uniform sieve size of 425 microns was selected across the three sample and subjected to investigation. The result for sample A shows that five phases where present in the ore which included; Ilmenite ($\text{Fe}_{1.10}\text{Ti}_{0.90}\text{O}_3$), Quartz (SiO_2), Albite ($\text{NaAlSi}_3\text{O}_8$), Spessartine ($\text{Mn}_3\text{Al}_2(\text{SiO}_4)_3$), Chlorite (NR) ($\text{Al} - \text{Fe} - \text{SiO}_2 - \text{O}$). With the complete details in the corresponding appendix result for XRF sample A, B and C.

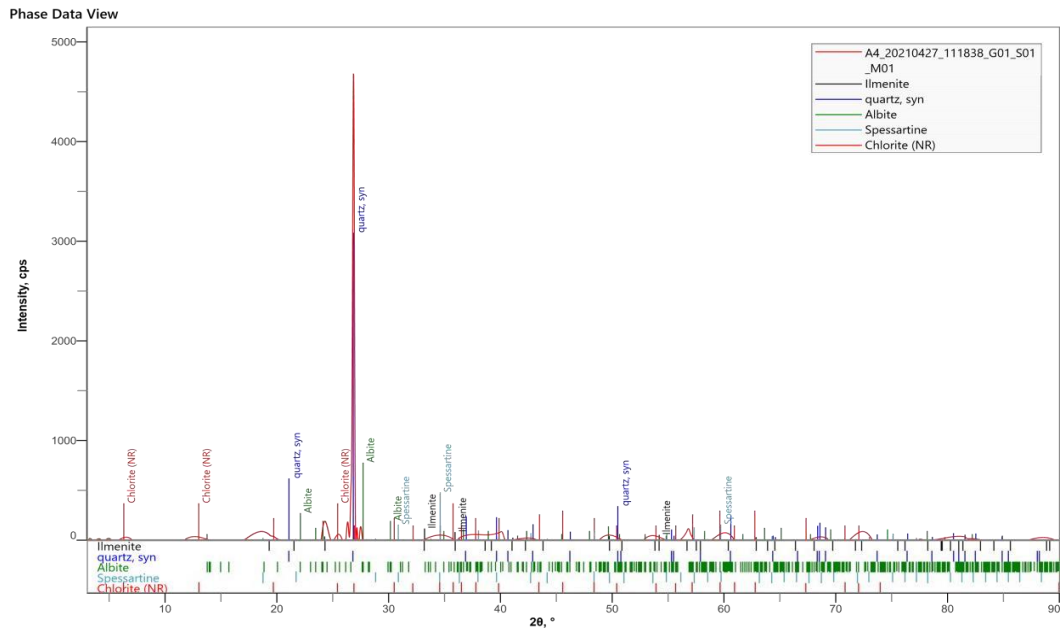


Figure 4.1: Sample A XRD result, showing the various diffraction peaks of Sample A ore minerals

The Figure 4.1 shows that Spessartine is the major manganese mineral and the Iron and Titanium spotted by the XRF was identified as Ilmenite, while Silicon as Quartz, aluminum found traces in Albite and Chlorite as the major gangue element. The peak noted that the intertwine of the gangue in the ore is due to the nature of formation. Other element could not be detected by the XRD as did the XRF due to the amount present or the amorphous nature therein.

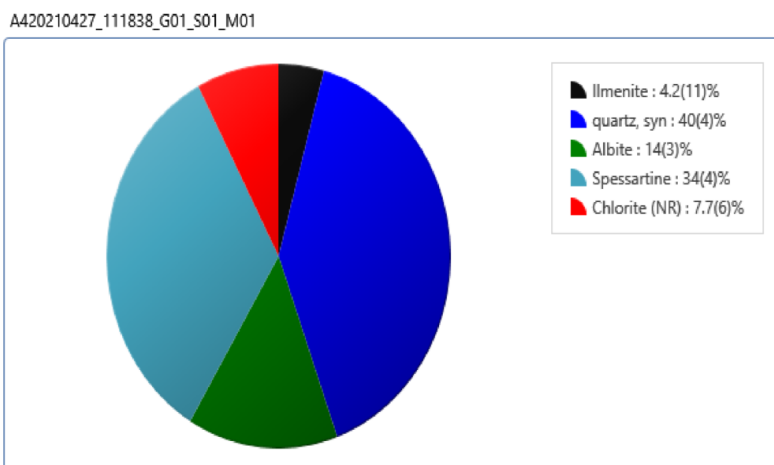


Figure 4.2: Pie Chart showing the phase percentage in Sample A

Figure 4.2 is a pie chart shows the percentage occupied by different phases as indicated in the XRF analysis of sample B, Spessartine and Quartz are the major phases as it occupies about 34% and 42% respectively. Since illmenite is paramagnetic, it concurs with the physical analysis that suggests magnetic separation for valuable recovery.

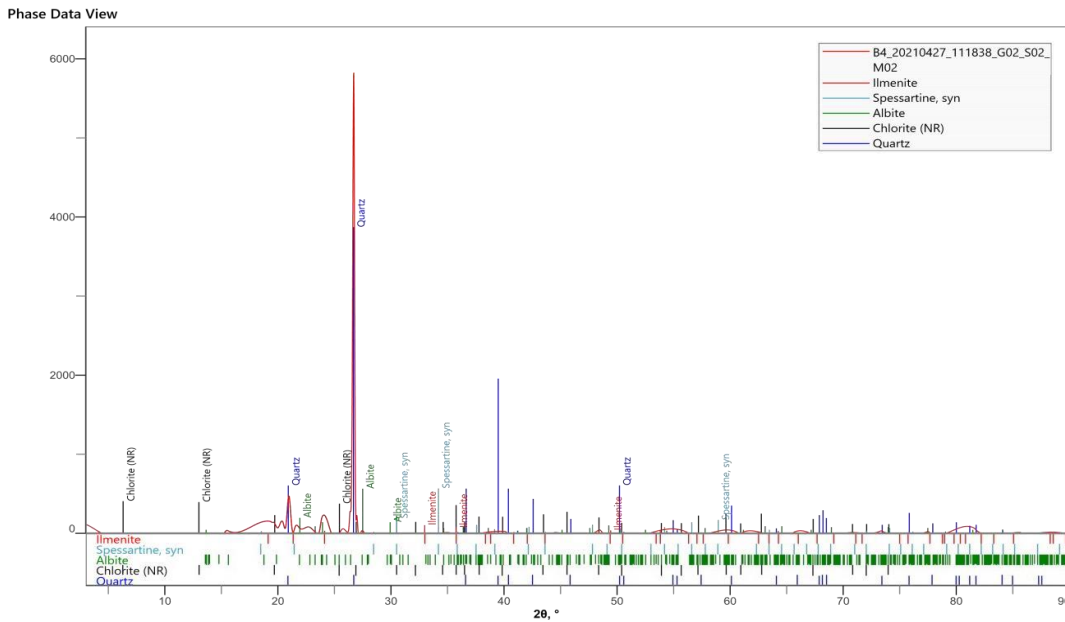


Figure 4.3: Sample B XRD result, showing the various diffraction peaks of the ore minerals

Sample B, Ilmenite $Fe_{1.04}Ti_{0.96}O_3$, Spessartine $Mn_3Al_2(SiO_4)_3$, Albite $NaAlSi_3O_8$, Chlorite (NR) $Al-Fe-SiO_2-O$, Quartz SiO_2 were detected and the combination of the element was same as stated for sample A as seen in Figure 4.1

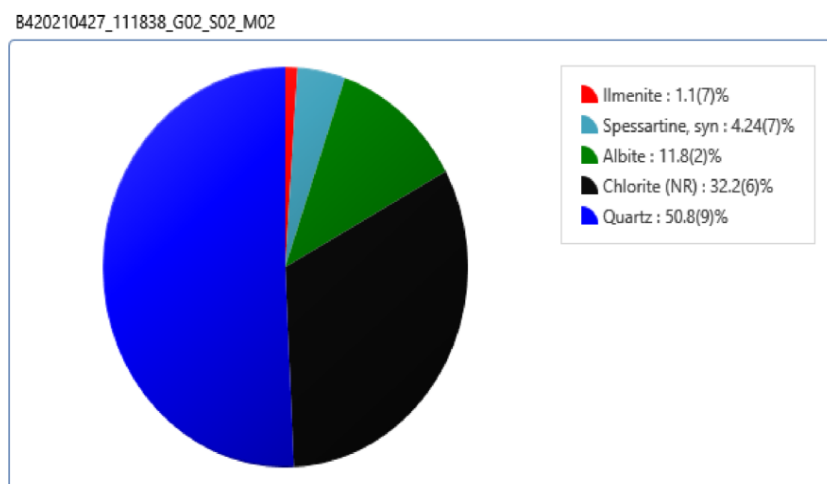


Figure 4.4: Pie Chart showing the phase percentage in Sample B

The Figure 4.3 shows the percentage of the constituent phases in the ore, quartz consumes the major percentage of the pie chart followed by chlorite. Although Spessartine was detected in little quantity, show it is a low-grade manganese ore

The Figure 4.5 below shows the peaks of the XRD result for sample C, the coloured lines shows different peaks identified and where matched to identify the different phases present in the ore.

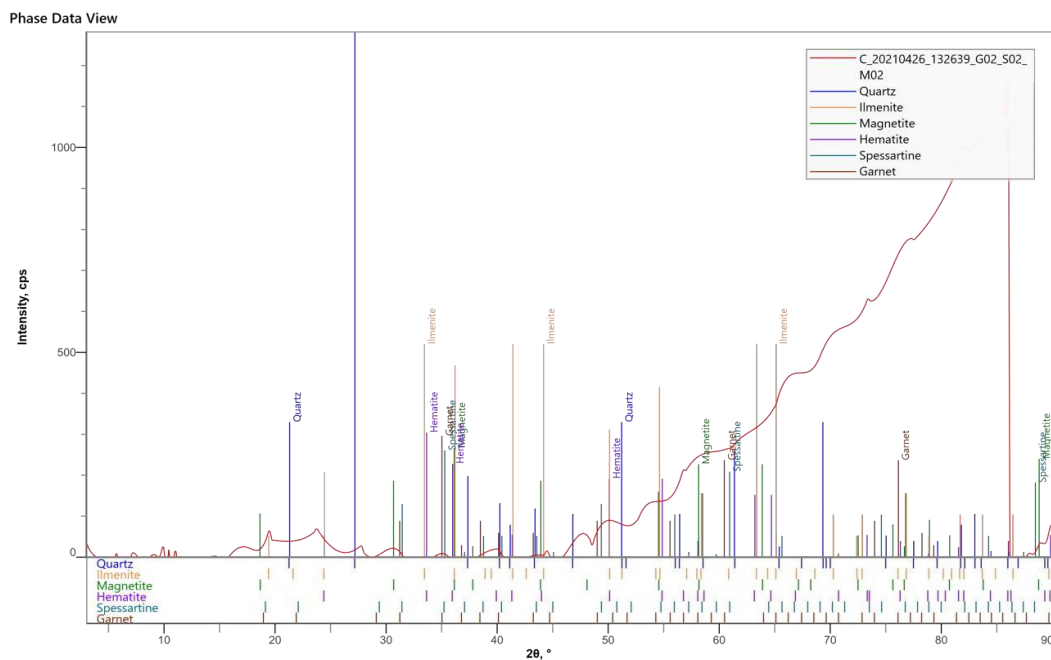


Figure 4.5: Sample C XRD result, showing the various diffraction peaks of the ore minerals

From the Figure 4.5, Six phases observed from the XRD characterisation of the sample C manganese ore, the include; Quartz Si O_2 , Ilmenite $\text{Fe} +2 \text{ Ti O}_3$, Magnetite $\text{Fe}_3 \text{ O}_4$, Hematite $\text{Fe}_2 \text{ O}_3$, Spessartine $\text{Mn}_3 \text{ Al}_2 (\text{Si O}_4)_3$, Garnet $3(\text{Ca, Fe, Mg}) \text{ O} \cdot (\text{Al, Fe})$ as seen in Figure 4.5. The weight percentage is presented in the Figure 4.6.

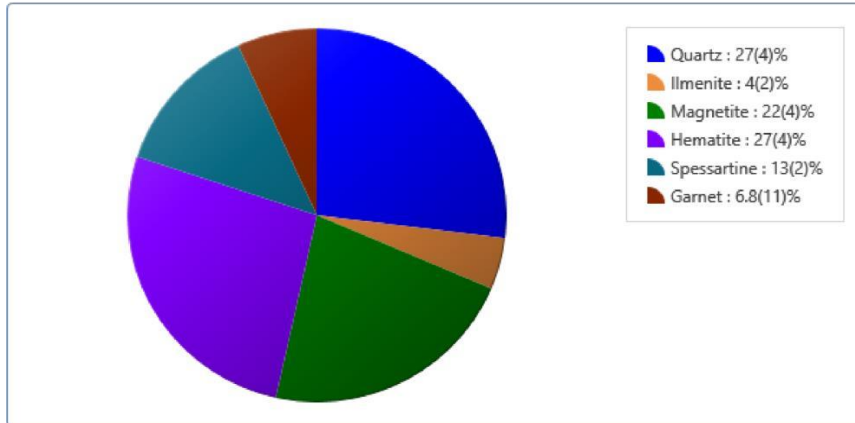


Figure 4.6: Pie Chart showing the phase percentage in Sample C

The percentage of the occurrence is represented on a pie chart as shown in the Figure 4.6, indicating that Hematite and Quartz and Magnetite occupies a greater percentage of the ore, which further validated the physical analysis carried out on a magnet, suggesting magnetic separation since most constituent of the ore are paramagnetic in properties.

4.3 X-ray Fluorescence (XRF) Spectroscopy

The XRF analysis was investigated for five different sieve sizes labelled A1 for 75 microns, A2 for 150 microns, A3 for 300 microns, A4 for 425 microns, and A5 for -75 microns. So also, B1 for 75 microns, B2 for 150 microns, B3 for 300 microns, B4 for 425 microns and B5 for -75 microns. Then, C1 for 75 microns, C2 for 150 microns, C3 for 300 microns, C4 for 425 microns and C5 for -75 microns. More details of the XRF analysis are shown in the appendix. Table 4.6 shows the XRF results for sample A,

Table 4.1: Sample A XRF result showing constituent elements.

Elements	Sample sizes				
	A1	A2	A3	A4	A5
Al ₂ O ₃ (%)	29.3157	28.7205	22.4469	24.9655	28.3157
SiO ₂ (%)	38.1840	40.5237	47.5631	40.9921	37.1840
P ₂ O ₅ (%)	0.1511	0.0773	0.1851	0.0991	0.1511

K₂O (%)	0.6001	0.5473	0.3137	0.4292	0.6001
CaO (%)	1.3480	1.1280	1.1920	1.2760	1.3480
V₂O₅ (%)	0.0070	0.0166	0.0079	0.0186	0.0070
MnO (%)	24.5785	23.4774	23.2532	25.7233	26.5785
Fe₂O₃ (%)	4.1261	3.9811	3.6387	4.5111	4.1261
CuO (%)	0.0090	0.0159	0.0150	0.0191	0.0090
As₂O₃ (%)	0.0314	0.0210	0.0000	0.0082	0.0314
Na₂O (%)	0.0144	0.0031	0.0141	0.0000	0.0144
Sb₂O₅ (%)	0.0415	0.0325	0.0276	0.0283	0.0415
BaO (%)	1.5758	1.4294	1.3170	1.9032	1.5758
PbO (%)	0.0174	0.0264	0.0256	0.0264	0.0174

The Table 4.1 shows the characterized ore was of high Alumina (26.75%), Silica (40.88%) and manganese (24.7%) averagely. With the focus on manganese across different sieve sizes shows that the liberation of manganese was more effective with the -75 microns (26.5785%). Indicating that greater percentage of manganese can be gotten if crushed to -75 microns. The high content of Alumina and Silica would require the use of other complex recovery to completely separate the manganese ore. The details of the result can be seen in the appendix A1 to A5 and is graphically presented in Figure 4.7.

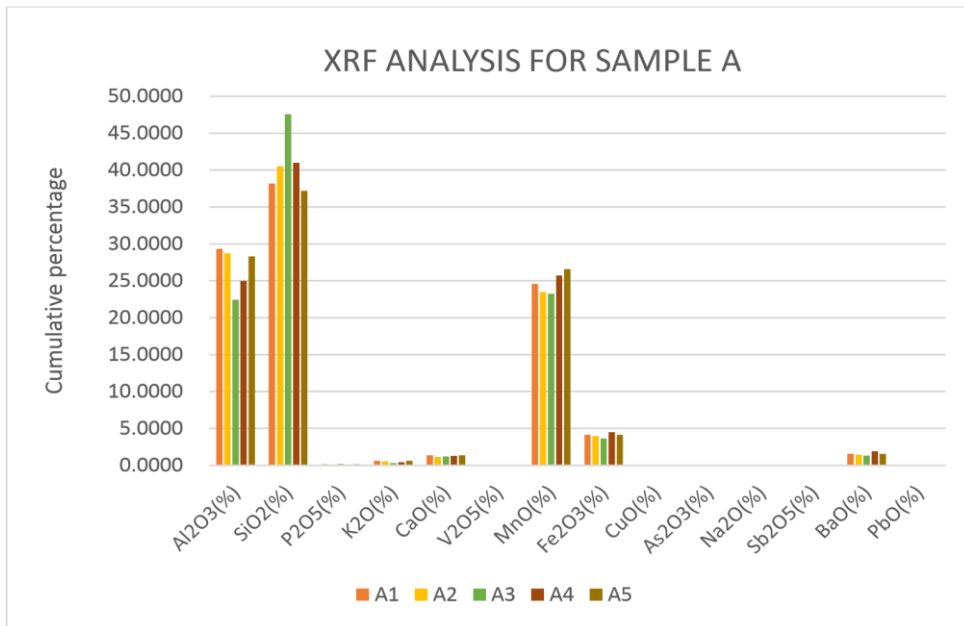


Figure 4.7: Variations of the element constituent Sample A.

The Figure 4.7 shows the graphical percentage of each sieve size with the different constituent of the ore. The sight of various other elements such as Al, Si, P, K, Ca, V, Mn, Fe, Cu, As, Na, Sb, Ba, Pb with their varied concentration would vest an added complicity to the recovery of Mn from the ore as posited by Sajjad et al., (2019) requiring other means of separating manganese valuables from the associated gangue.

The Table 4.2 shows the XRF result for the sample B, indicating the content of the ore in percentage for the five sieve mesh sizes investigated.

Table 4.2: Sample B XRF result showing constituent elements

Elements	Sample Sizes				
	B1	B2	B3	B4	B5

Al₂O₃ (%)	23.5664	22.9529	23.2066	23.2066	26.3653
SiO₂ (%)	32.0687	33.8407	35.1130	35.2130	28.8374
P₂O₅ (%)	0.1417	0.1474	0.1646	0.1646	0.1737
K₂O (%)	0.3592	0.4469	0.4705	0.4705	0.5060
CaO (%)	3.8520	3.8302	3.3825	3.3825	4.7179
TiO₂ (%)	0.0000	0.0000	0.0000	0.0000	0.1580
MnO (%)	35.8720	35.0250	33.1231	33.0231	34.8338
Fe₂O₃ (%)	3.2149	2.7300	3.7087	3.7087	3.6079
Na₂O (%)	0.0233	0.0302	0.0260	0.0260	0.0344
Sb₂O₅ (%)	0.0043	0.0069	0.0209	0.0209	0.0264
BaO (%)	0.8974	0.9896	0.7842	0.7842	0.7393

The XRF for sample B also showed Aluminum (23.5664%), Silicon (32.0687%), and manganese (35.8720%) where characterized in high grades as shown in Table 4.2. The liberation in manganese showed better result with the 75 microns retained.

Suggesting that other mineralogical extraction would be more effective if the ore is crushed to size 75 microns.

Figure 4.8 shows the graphical representation of the Table 4.7 to further buttress the result.

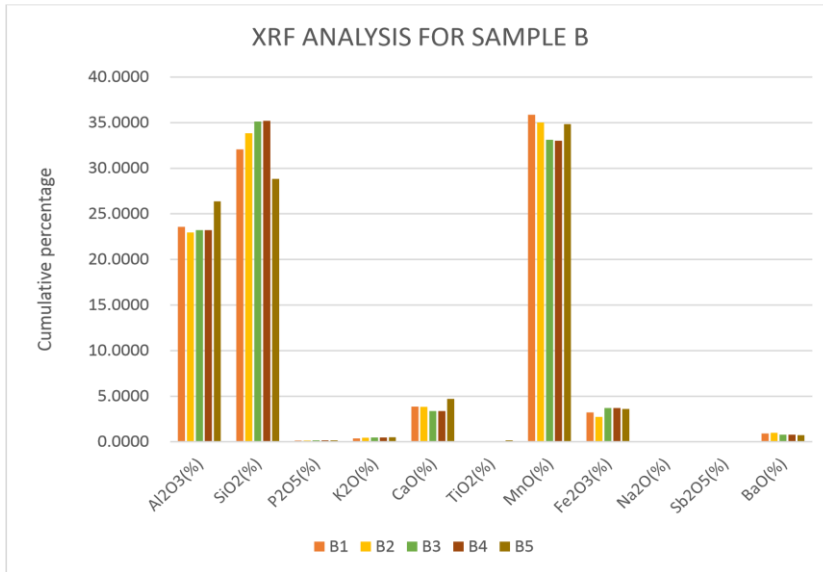


Figure 4.8: Variations of the element constituent of Sample B

The Figure 4.8 shows the percentage of each sieve size with the different constituent of the ore. A more detailed result is shown in the appendix B1 to B5. The sight of various other elements such as Al, Si, P, K, Ca, Ti, Fe, Na, Sb, Ba, with their varied concentration especially silica and Aluminum which depict a high percentage presence and may tend to be an added complicity to the recovery of Mn from the ore (Sajjad *et al.*, 2019). Some other elements are found in traces and can easily be separated.

The Table 4.8 shows the XRF result for sample C and reveals the individual elemental percentage in the ore and suggest the rate at which liberation has occurred after been crushed into different sizes.

Table 4.3: Sample C XRF result showing constituent elements

Elements	Sample Sizes
----------	--------------

	C1	C2	C3	C4	C5
Al₂O₃(%)	30.6286	32.0438	33.8747	27.8337	32.0965
SiO₂ (%)	41.4684	44.1720	38.2760	45.7933	38.3415
P₂O₅ (%)	0.2186	0.2138	0.2295	0.2145	0.2262
K₂O (%)	0.0442	0.1226	0.0491	0.1636	0.0000
CaO (%)	2.2202	1.7240	2.0961	1.6120	2.2011
TiO₂ (%)	0.4003	0.3539	0.6223	0.7309	0.7537
MnO (%)	16.3266	13.5566	16.0513	14.6113	17.3129
Fe₂O₃(%)	8.6931	7.8065	8.8010	8.9826	9.0682
Na₂O (%)	0.0000	0.0056	0.0000	0.00000	0.0000
Ag₂O(%)	0.0000	0.0012	0.0000	0.0027	0.0000
NiO (%)	0.0000	0.0000	0.0000	0.0290	0.0000
MoO₃(%)	0.0000	0.0000	0.0000	0.0095	0.0000
BaO (%)	0.0000	0.0000	0.0000	0.0168	0.0000

The XRF result for sample C, showed different constituent as presented in the Table and their percentages vividly illustrated in the Figure 4.9. The result indicated high percentage of Aluminum, Silicon, Manganese and Iron. With varying manganese percentage across sieve sizes, but the sieve size of -75 microns, having the highest liberation rate and there suggesting that beneficiation and other metallurgical processes would better achieve high manganese if crushed to this sieve size. Appendix C1 to C5 contains a detailed result of the XRF analysis of sample C ore.

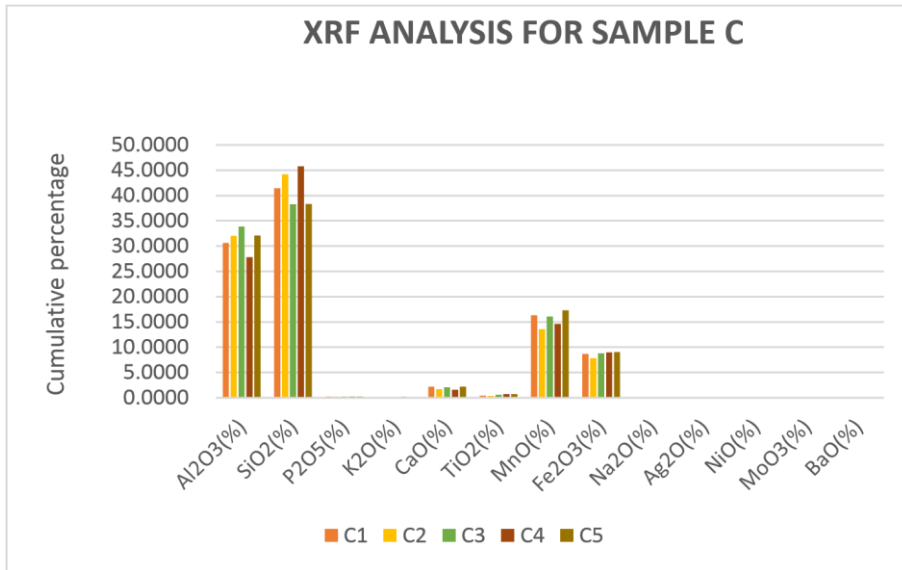


Figure 4.9: Variations of the element constituent of Sample C

The percentage of manganese present in this ore is low from the Figure 4.9, this is a result of the condition with which the mineral formation happened compounded by other related mechanism may be responsible for the relative smaller amount of manganese spotted in the ores. Many other elements are found in their traces while some other could not be capture because of the negligible percentage of their occurrence.

4.4 Sieve Analysis

The Table 4.4 shows the test result for the screen test, with the cumulative percentage passing and the cumulative percentage retained in the sieve for each screen size. Once the weight in each sieve was ascertained, simple calculations were used to determine the weight retained, cumulative percentage passing and the cumulative percentage retained. The cumulative percent passing and cumulative percent retained against the various sieve sizes used was plotted and shown in Figure 4.10

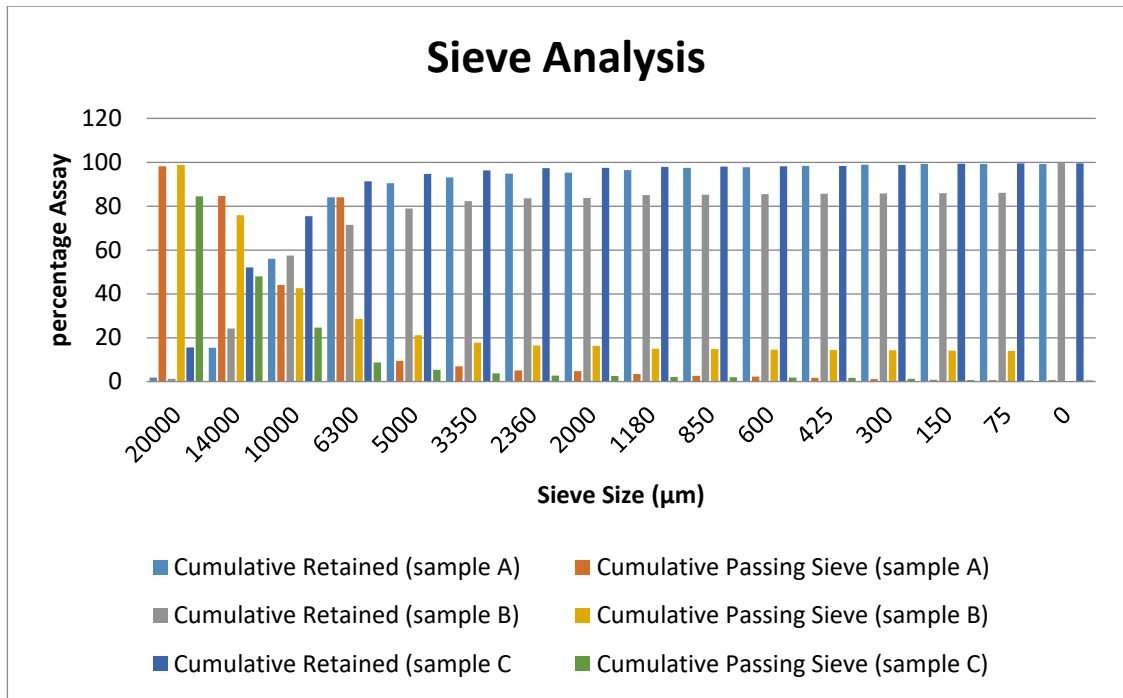


Figure 4.10: Variations of the sieve analysis

The cumulative retained for sample A, B and C for the sieve sizes of 425µm was 98.92, 85.76 and 98.73, while that for 300 µm was 99.15, 85.95 and 99.32, the sieve mesh of 150 µm was 99.25, 86.05 and 99.47, and the -75 µm was 99.26, 99.71 and 99.48 respectively. The analysis allowed for selection of this mesh sizes from the different ores to be subjected to the various analysis required to arrive at the expected outcome of this research.

Table 4.4: Results for sieve analysis

Sieve Size (µm)	Weight Retained			Percentage Retained			Cumulative Retained			Cumulative Passing		
	A	B	C	A	B	C	A	B	C	A	B	C
+20000	181.4	56.76	4201.2	1.89	1.29	15.56	1.89	1.29	15.56	98.11	98.71	84.44
-20000+14000	1299.8	1008.48	9860.4	13.54	22.92	36.52	15.43	24.21	52.08	84.57	75.79	47.92
-14000+10000	3897.6	1460.8	6299.1	40.6	33.2	23.33	56.03	57.41	75.41	43.97	42.59	24.59
-10000+6300	2688	619.08	4301.1	28	14.07	15.93	84.03	71.48	91.34	84.07	28.52	8.66
-6300+ 5000	620.2	324.72	899.1	6.46	7.38	3.33	90.49	78.86	94.67	9.51	21.14	5.33
-5000+ 3350	246.72	149.16	434.7	2.57	3.39	1.61	93.06	82.25	96.28	6.94	17.75	3.72
-3350+ 2360	174.72	57.1	259.2	1.82	1.29	0.96	94.88	83.54	97.24	5.12	16.46	2.76
-2360+ 2000	33.6	10.12	56.7	0.35	0.23	0.21	95.23	83.77	97.45	4.77	16.23	2.55
-2000+ 1180	120.96	57.1	121.5	1.26	1.29	0.45	96.49	85.06	97.9	3.51	14.94	2.1
-1180+ 850	86.4	6.16	29.70	0.90	0.14	0.11	97.39	85.2	98.01	2.61	14.8	1.99
-850+ 600	35.52	9.24	35.1	0.37	0.21	0.13	97.76	85.41	98.14	2.24	14.59	1.86
-600+ 425	55.68	10.56	40.5	0.58	0.24	0.15	98.34	85.65	98.29	1.66	14.35	1.71

Sieve Size (μm)	Weight Retained			Percentage Retained			Cumulative Retained			Cumulative Passing		
-425+ 300	56.10	4.84	118.8	0.58	0.11	0.44	98.92	85.76	98.73	1.08	14.24	1.27
-300+ 150	22.08	8.36	159.3	0.23	0.19	0.59	99.15	85.95	99.32	0.85	14.05	0.68
-150+ 75	9.6	4.4	40.5	0.10	0.10	0.15	99.25	86.05	99.47	0.75	13.95	0.53
-75	0.96	6010.4	2.7	0.01	13.66	0.01	99.26	99.71	99.48	0.74	0.29	0.52

4.5 Mineral Liberation

Quantitative analysis carried out on the samples was used to measure the characteristics of manganese liberated from the ores.

The formula used for this was:

$$\text{Degree of liberation using Quantitative analysis } Y = \frac{(\sum T_i - \sum G_i) \times C}{\sum T_i}$$

Where $\sum T_i$ = The sum total of the constituent of the mineral ore

$\sum G_i$ = The sum total of the gangue

C = Liberation multiplying constant

Y = The degree of liberation

i = The test sieve size

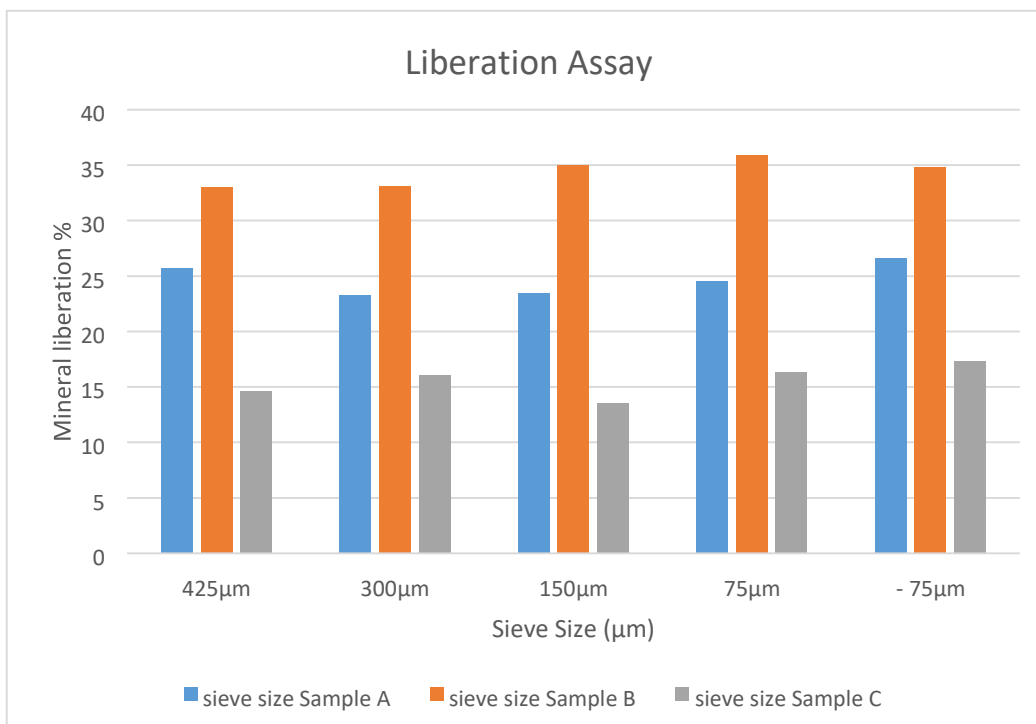


Figure 4.11: Liberation Assay of Manganese Sample A-C

From the Figure 4.11, it was also observed that liberation can be attained at grinding. For sample A approximately 25% of liberation was observed in $-75\mu\text{m}$ while a decrease was observed in larger sieve size expect for the $425\mu\text{m}$ which showed good potential also. For sample B, 35% liberation was observed, for a range of sieve size $-75\mu\text{m}$, $75\mu\text{m}$, $150\mu\text{m}$, after which decrease was then observed so also with sample C, showing the best liberation was in the $-75\mu\text{m}$. By and large the smaller the sample size ground, the better the liberation.

4.6 Work Index Calculations

Table 4.5a and 4.5b presents the size analysis of particles fed and also discharged from the ball mill respectively for granite which was used as a reference ore. Whilst Table 4.6a and 4.6b, 4.7a and 4.7b, 4.8a and 4.8b presents the distribution of particle size feed and discharged from the ball mill for manganese (Test Ore) for three different samples A, B, C respectively. The Tables were used to calculate the feeds and passing product at 80% for both the reference ore (granite) and the test ore (Manganese) for sample A, B, C. the work index for sample A was found to be 4.3kwh/ton, while that of sample B and C was 2.4kwh/ton and 2.0 kwh/ton respectively. This value showed a manganese ore of grade B. variations are displayed in Figure 4.12a, 4.12b, 4.13a, 4.13b, 4.14a, 4.14b, 4.15a, 4.15b respectively.

Table 4.5a: Sieve Size of particle (reference ore) feed to ball mill

Sieve Size(μm)	Weight (g)	Weight Retained (%)	Cumulative Weight Retained (%)	Cumulative Weight Passing (%)
+1400	11.53	11.54	11.54	88.46
+1000	12.22	12.23	23.77	76.23
+710	13.88	13.89	37.66	62.34
+500	13.94	13.96	51.62	48.38
+355	12.36	12.37	63.99	36.01
+250	10.66	10.67	74.66	25.34
+180	9.97	9.98	84.64	15.36
+125	4.64	4.65	89.29	10.71
+90	3.96	3.96	93.25	6.75
+63	2.98	2.98	96.23	3.77
-63	3.75	3.75	99.98	0.02

Iterating

$$\text{If } 1400\mu\text{m} = 88.64$$

$$X\mu\text{m} = 80\% \tag{18}$$

Then,

$$X\mu\text{m} = \frac{1400 \times 80}{88.64} = 1263.54\mu\text{m} - F_r$$

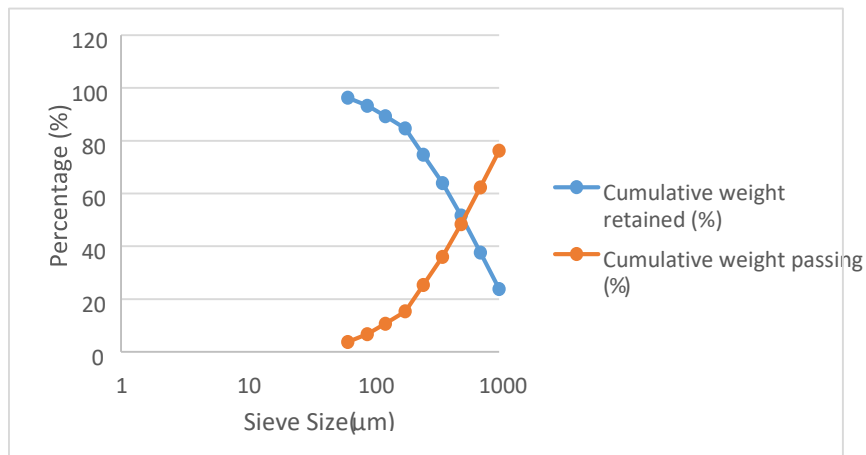


Figure 4.12a: A variation of sieve size against cumulative passing and cumulative retained of granite reference ore

Table 4.5b: Reference ore particle size discharged from the ball mill

Sieve Size(μm)	Weight (g)	Weight Retained (%)	Cumulative Weight Retained (%)	Cumulative weight Passing (%)
-----------------------------	------------	---------------------	--------------------------------	-------------------------------

+710	21.09	21.11	21.11	78.89
+500	16.94	16.96	38.07	61.93
+355	22.56	22.59	60.66	39.34
+250	16.52	16.54	77.2	22.8
+180	7.97	7.98	85.18	14.82
+125	5.97	5.98	91.16	8.84
+90	4.29	4.30	95.46	4.54
+63	2.97	2.97	98.43	1.57
-63	1.57	1.57	100	0.00
	99.88			

If $710\mu\text{m} = 78.89$

$X\mu\text{m} = 80\%$

Then,

$$X\mu\text{m} = \frac{710 \times 80}{78.89} = 719.99\mu\text{m} - P_r$$

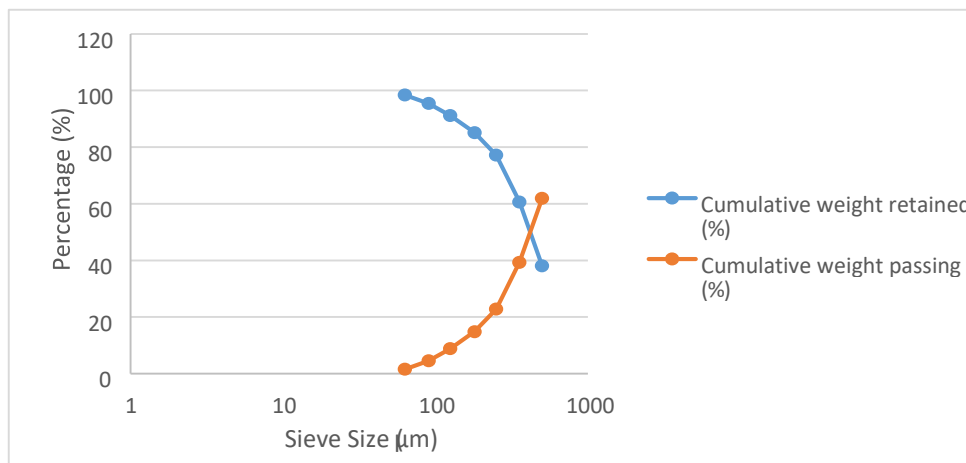


Figure 4.12b: Variation of sieve size against cumulative passing and cumulative retained of granite (reference ore) product from ball mill

Table 4.5a and Figure 4.12a Infers the result acquired for the fractional sieve sizes feed into the ball mill and the graph showing the 50% intersection signifying optimal size of grinding to obtain liberation sizes.

Table 4.6a: Sieve Size of particle (Test ore Sample A) feed to ball mill

Sieve Size(μm)	Weight (g)	Weight Retained (%)	Cumulative Weight Retained (%)	Cumulative Weight Passing (%)
-----------------------------	------------	---------------------	--------------------------------	-------------------------------

+710	23.40	23.43	23.43	76.57
+500	29.94	29.98	53.41	46.59
+355	19.56	19.59	73.00	27.00
+250	8.84	8.85	81.85	18.15
+180	6.88	6.89	88.74	11.26
+125	4.42	4.43	93.17	6.83
+90	3.96	3.96	97.13	2.87
+63	1.42	1.38	98.51	1.49
-63	1.44	1.42	99.93	0.07

If $710\mu m = 76.57$

$X\mu m = 80\%$

Then,

$$X \mu m = \frac{710 \times 80}{76.57} = 741.80\mu m - F_t$$

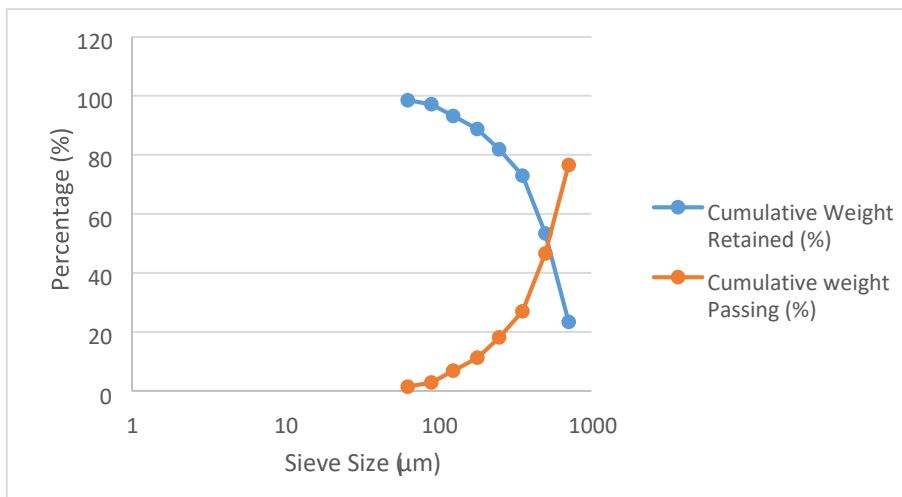


Figure 4.13a: Variation of sieve size against cumulative passing and cumulative retained of Manganese ore sample A feed to ball mill

Table 4.6b: Test ore particle size discharged from the ball mill Sample A

Sieve size (μm)	weight retained (g)	Weight retained (%)	Cumulative weight retained (%)	Cumulative weight passing (%)
+710	10.20	10.22	10.22	89.78
+500	9.67	9.69	19.9	80.1
+355	8.72	8.74	28.64	71.36
+250	37.73	37.8	66.44	33.56

+180	13.32	13.34	79.78	20.22
+125	6.82	6.8	86.58	13.42
+90	6.70	6.7	93.28	6.72
+63	3.85	3.86	97.14	2.86
-63	2.80	2.81	99.95	0.05

If $710\mu m = 89.78$

$X\mu m = 80\%$

Then,

$$X\mu m = \frac{710 \times 80}{89.78} = 632.66\mu m - P_t$$

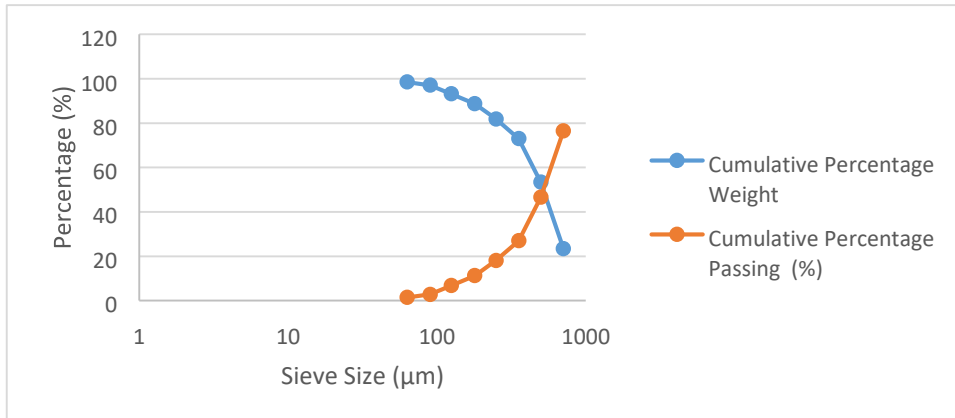


Figure 4.13b: Variation of sieve size against cumulative passing and cumulative retained of Manganese ore sample A product from ball mill

Table 4.6a and Figure 4.13a Infers the result acquired for the fractional sieve sizes feed into the ball mill and the graph showing the 50% intersection signifying optimal size of grinding to obtain liberation sizes.

Using Bond's equation;

$$W_r = W_t = W_{ir} \frac{\left[\frac{10}{\sqrt{P_r}} - \frac{10}{\sqrt{F_r}} \right]}{\left[\frac{10}{\sqrt{P_t}} - \frac{10}{\sqrt{F_t}} \right]}$$

Where,

W_r = Work index of reference ore

W_t = Work index of test ore

P_r = Product of reference ore diameter, 80% passing through the sieve aperture

P_t = Product of Test ore diameter, 80% passing through the sieve aperture

F_r = Feed of reference ore diameter, 80% passing through the sieve aperture

F_t = Feed of Test ore diameter, 80% passing through the sieve aperture

$$W_r = 14.39 \left[\frac{\frac{10}{\sqrt{719.99}} - \frac{10}{\sqrt{1263.54}}}{\frac{10}{\sqrt{632.66}} - \frac{10}{\sqrt{741.80}}} \right] = 4.3 \text{ Kw.h/ton}$$

Table 4.7a: Sieve Size of particle (Test ore Sample B) feed to ball mill

Sieve Size(μm)	Weight (g)	Weight Retained (%)	Cumulative Weight Retained (%)	Cumulative Passing (%)
+710	20.40	20.43	20.43	79.57
+500	25.74	25.78	46.21	53.79
+355	9.56	9.58	55.79	44.21
+250	12.54	12.56	68.35	31.65
+180	16.88	16.91	85.26	14.74
+125	5.82	5.83	91.09	8.91
+90	4.96	4.96	96.05	3.95
+63	2.42	2.42	98.47	1.53
-63	1.52	1.52	99.99	0.01

If $710\mu\text{m} = 79.57$

$X\mu\text{m} = 80\%$

Then,

$$X \mu\text{m} = \frac{710 \times 80}{79.57} = 713.84\mu\text{m} - F_t$$

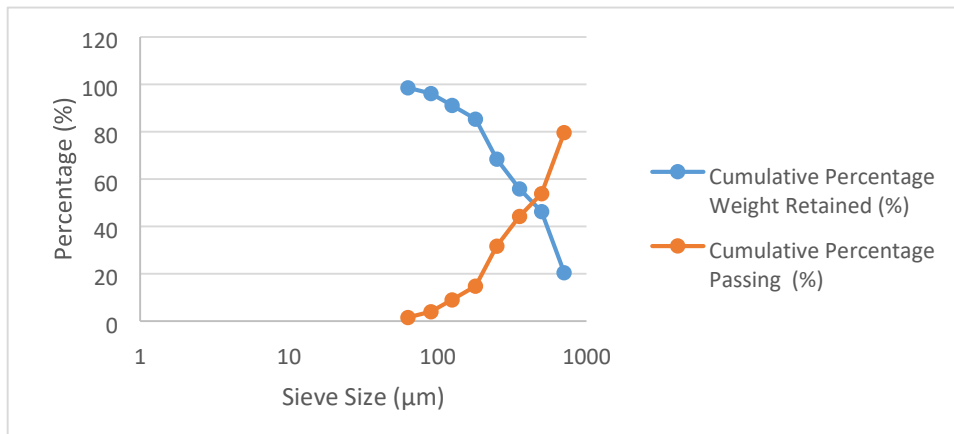


Figure 4.14a: Variation of sieve size against cumulative passing and cumulative retained of Manganese ore sample B feed to ball mill

Table 4.7b: Test ore particle size discharged from the ball mill sample B

Sieve size (μm)	weight retained (g)	Weight retained (%)	Cumulative weight retained (%)	Cumulative weight passing (%)
+710	11.93	11.94	11.94	88.06
+500	14.56	14.58	26.52	73.48
+355	10.72	10.73	37.25	62.25
+250	25.23	25.25	62.50	37.5
+180	17.44	17.46	79.96	20.04
+125	6.82	6.83	86.79	13.21
+90	7.09	7.10	93.89	6.11
+63	3.55	3.55	97.44	2.56
-63	2.55	2.55	99.99	0.01

$$\text{If } 500\mu\text{m} = 88.60$$

$$X\mu\text{m} = 80\%$$

Then,

$$X\mu\text{m} = \frac{500 \times 80}{73.48} = 544.37\mu\text{m} - P_t$$

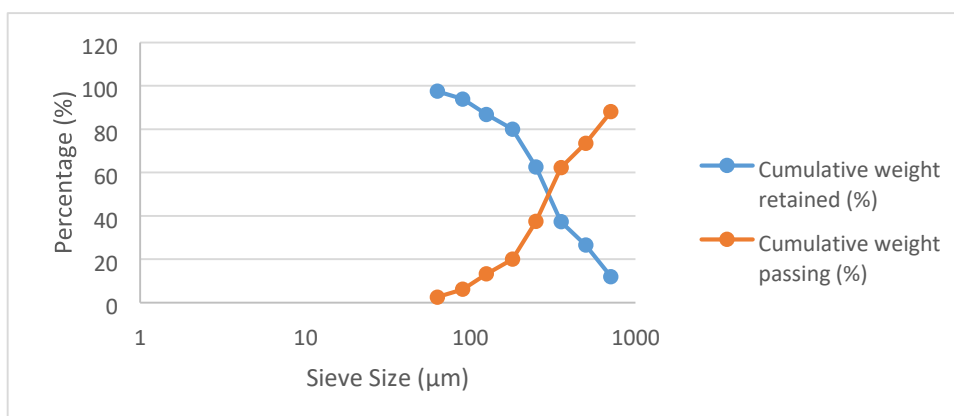


Figure 4.14b: Variations of sieve size against cumulative passing and cumulative retained of Manganese ore sample B product from ball mill

Table 4.7a and Figure 4.14a Infers the result acquired for the fractional sieve sizes feed into the ball mill and the graph showing the 50% intersection signifying optimal size of grinding to obtain liberation sizes.

Then,

$$W_r = 14.39 \left[\frac{\frac{10}{\sqrt{719.99}} - \frac{10}{\sqrt{1263.54}}}{\frac{10}{\sqrt{544.37}} - \frac{10}{\sqrt{713.84}}} \right] = 2.4 \text{ kw.h/ton}$$

Table 4.8a: Sieve Size of particle (Test ore Sample C) feed to ball mill

Sieve Size(μm)	Weight (g)	Weight Retained (%)	Cumulative Weight Retained (%)	Cumulative Weight Passing (%)
+710	23.88	23.91	23.91	76.09
+500	18.94	18.96	42.87	57.13
+355	17.14	17.16	60.03	39.97
+250	15.42	15.44	75.47	24.53
+180	9.57	9.58	85.05	14.95
+125	5.44	5.45	90.5	9.5
+90	3.96	3.96	94.46	5.54
+63	2.98	2.98	97.44	2.56
-63	2.55	2.55	99.99	0.01

If $710\mu\text{m} = 76.09$

$X_{\mu\text{m}} = 80\%$

Then,

$$X_{\mu\text{m}} = \frac{710 \times 80}{76.09} = 746.48\mu\text{m} - F_t$$

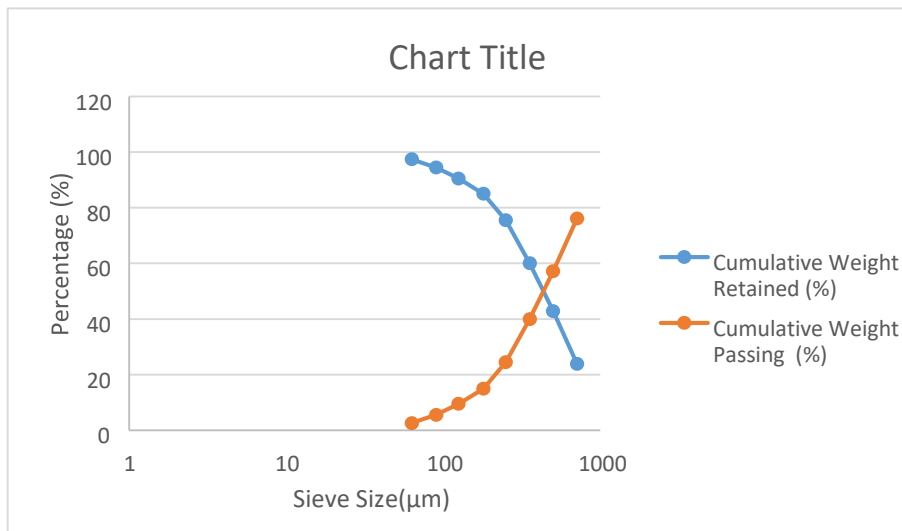


Figure 4.15a: Variations of sieve size against cumulative passing and cumulative retained of Manganese ore sample C feed to ball mill

Table 4.8b: Test ore particle size discharged from the ball mill sample C

Sieve size (µm)	weight retained (g)	Weight retained (%)	Cumulative weight retained (%)	Cumulative weight passing (%)
+710	20.42	20.44	20.44	79.56
+500	14.33	14.34	34.78	65.22
+355	11.32	11.33	46.11	53.89
+250	22.41	22.43	68.54	31.46
+180	14.21	14.22	82.76	17.24
+125	6.82	6.83	89.59	10.41
+90	5.88	5.89	95.48	4.52
+63	3.44	3.44	98.92	1.08
-63	1.08	1.08	100	0.00

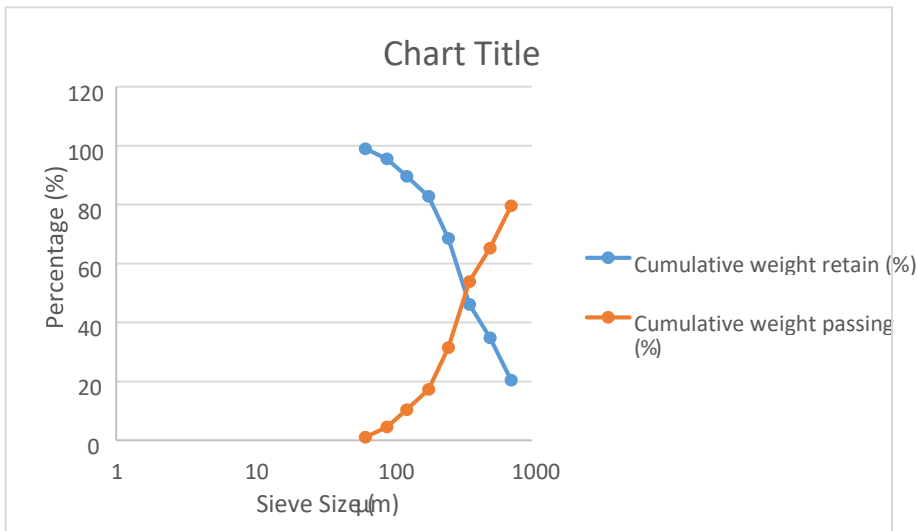


Figure 4.15b: Variations of sieve size against cumulative passing and cumulative retained of Manganese ore sample C product from ball mill

Table 4.1a and Figure 4.15a Infers the result acquired for the fractional sieve sizes feed into the ball mill and the graph showing the 50% intersection signifying optimal size of grinding to obtain liberation sizes.

$$\text{If } 710\mu\text{m} = 79.56$$

$$X\mu\text{m} = 80\%$$

Then,

$$X\mu\text{m} = \frac{710 \times 80}{79.56} = 713.93\mu\text{m} - P_t$$

Then,

$$W_r = 14.39 \left[\frac{\frac{10}{\sqrt{719.99}} \frac{10}{\sqrt{1263.54}}}{\frac{10}{\sqrt{713.93}} \frac{10}{\sqrt{746.48}}} \right] = 2.0 \text{ kw.h/ton}$$

4.7 Physical Analysis

The result of the physical analysis of the ores are presented and discussed.

4.7.1 Hand specimen: The three samples had black colour with traces of brownish spot around it. This indicates the presence of iron. The samples were also tested for physical attraction to magnet and all three samples showed some level of attraction to the magnet, this indicated that the samples could be upgraded using magnetic separator.

4.7.2 Density determination: The density of each of the three samples was ascertained and the result presented in Figure 4.12, sample A was 7750g/ml while sample B was 7733g/ml and Sample C was 7710g/ml.

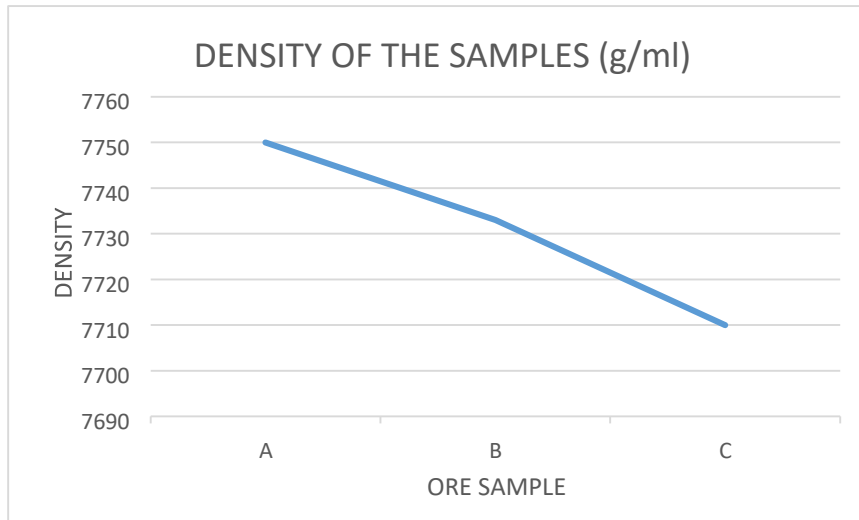


Figure 4.16: Variation of the density of the three samples

The Figure 4.16 is the graphical representation of the densities of the three samples, indicating the density of sample A to be 7750g/ml, sample B 7730g/ml and sample C 7710g/ml, sample A was found to be denser than the other samples. Since most separating method employs the difference in the density of ore to determine the agent use in concentration, it is pertinent that the density of the ore be ascertained.

CHAPTER FIVE

5.0 CONCLUSION AND RECOMMENDATIONS

5.1 Conclusion

Three ore from Ka'oje in Kebbi State, Madaka in Niger State and Akampa in Cross river State were characterized, however the intricacies in the ores are rooted in the Mn-Al-Fe-Si affiliations (determined through XRD), with strata of intergrowth and disseminated zoning as revealed by the SEM. These structures are noticed in the irregular granular shape the sample B showed although quite sparse in A and C. The major elemental constituent was revealed to be Al, Si, Mn and Fe in sample A, Al, Si, Mn, Ca and Fe in sample B and C. while various elements suchlike K, Pb, Ba, Ti were also identified negligible amount. The XRD investigation disclosed that the samples were chiefly Spessartine ($Mn_3 Al_2 (Si O_4)_3$) and Iron

rich Ilmenite this supports the XRF result of the major constituent being Al, Si, Mn and Fe.

The structure and phases present shows complexity of the ore indicating that the formation of the ore have been greatly influenced by the composition of the parent rock.

The liberation of the ore was attained at grinding, for sample A approximately 25% of liberation was observed in -75 μ m while a decrease was observed in larger sieve size expect for the 425 μ m which showed good potential also. For sample B, 35% liberation was observed, for a range of sieve size -75 μ m, 75 μ m, 150 μ m, after which decrease was then observed so also with sample C showing the best liberation was in the -75 μ m. By and large the smaller the sample size grinded the better the liberation.

The work index of the three manganese ores were calculated to be 4. 3kw.h/ton, 2. 4kw.h/ton and 2. 0kw.h/ton respectively for Sample A, B and C

The three samples had black colour with traces of brownish spot around it indicating the presence of iron. All three samples showed some level of attraction to the magnet, this indicating that the samples could be upgraded using magnetic separator.

The density of each of the three samples was ascertained to be sample A was 7750g/ml while sample B was 7733g/ml and Sample C was 7710g/ml respectively.

5.2 Recommendations

1. From the findings of this research, it was observed that manganese which was predominantly Spessartine is associated with alumina and silica. It is therefore recommended that other separation technique be used for effective recovery of manganese mineral.

2. Other deposit in the country should be characterized to determine which deposits would be efficient for value addition and economic emancipation.
3. Access to the deposit sites should be granted easily for research purposes and funding be made available to execute a more robust and holistic research.

5.3 Contributions to Knowledge

1. The characterization of three deposits of manganese ores were achieved revealing the ores to be spessartine and having three distinct morphology.
2. An effective liberation size was achieved of below 75 microns as 25%, 35% and 20% fines were recovered from locally available manganese.
3. The optimal size grade was obtained with work index and energy value utilized peaked at 4.3 kWh/t, 2.4 kWh/t and 2.0 kWh/t respectively

REFERENCE

- Andrei, A. B., Elena, G. U., Hassan, Y. A. (2015). X-Ray Diffraction: Instrumentation and Applications, *Critical Reviews in Analytical Chemistry*, 45(4), 289-299
- Akintola, O.A (2019). Geological map of Nigeria showing occurrences of manganese deposits. *Asian Journal of Geographical research*.
- Alessio, L., Campagna, M., Lucchini, R. (2007). From Lead to Manganese through Mercury: Mythology, science, and lesson for prevention. *American Journal of Industrial Medicine* 50 (11), 779-787.

- Berry, T. F., and Bruce, R. W. (1996). A simple Method of Determining the Grindability of Ores, *Can, Min Journal*, 63, 15-16.
- Bond, F.C. (1996). The theory of Comminution transaction of America institute of mining Engineers, 193,
- Dell, R.M. (2000). Batteries fifty years of material development; *Solid States Ionics* .134 (1-2), 139-158.
- Donskoi, E., Suthers, S.P., Campbell, J.J., Raynlyn, T., (2008). Modelling and Optimization of hydrocyclone for iron ore fines beneficiation- using optical imagine analysis and iron ore texture classification. *Int. J Miner. Process.* 87,106-119.
- Duroudier, J. (2016). Size Reduction of Divided Solids, *Elsevier Publication*, 1, 73-97
- Gupta, A., and Yan, D. S. (2006). Mineral Processing Design and Operation- An Introduction, 1, 128-141
- Gaudin, A.M. (1939). *Principles of Mineral Dressing*. New York: McGraw-Hill.
- Gay, S.L. (2004). Simple texture-based liberation modelling of ores; *Minerals Engineering* 17, 1209–1216.
- Gbadamosi, Y.E., Alabi O.O., Ola-Omole, O.O., Adetula, Y.V. (2021). Petrological, , and Chemical Mineralogical Characterisation of Anka (Zamfara State) Manganese Ore; *NanoNEXT* 2(1), 7-12.
- Gy, P.M. (1979). Sampling of particulate material: Theory and practice. *Elsevier scientific Pub. Co. Amsterdam*.
- Halder, S. (2018). *Mineral Exploration Principles and Applications*. Elsevier Science and Technology Book. 2, 259-290
- Hamid, S.A., Alfonso, P., Oliva, J., Anticoi, H., Guasch, E., Sampaio, C H., Garcia Vallès, M., and Escobet, T. (September 2019). Modelling the Liberation of Comminuted Scheelite Using Mineralogical Properties. *MDPI Academic open Access Publishing*.
- Hassan, B. (2013). Upgrading of Wasagu Manganese Ore to Metallurgical Grade Concentrate. Unpublished M.Sc Thesis, *Ahmadu Bello University, Zaria*, 1-66
- Jones, M.P. (2000): Principle of Minerals Flotation. *Australasia Inst. Min. Metallurgy, Victoria*.
- Karl, W., Macalester, C., and Andy, B. (2011). X-Ray Fluorescence (XRF), Geochemical and Instrumentation Analysis;
- King, R.P. (1979). A model for quantitative estimation of mineral liberation by grinding; *Int. J. Min. Process.* 6, 207–220.

- King, R.P (2012). Modelling and Simulation of Mineral Processing Systems; *Society for Mining, Metallurgy, and Exploration, Inc. (SME): Englewood, CO, USA*, 55–96.
- Lingyun Y, Zhucheng .H, Tao. J, Peng. Z, Ronghai. Z, and Zhikai L. (2017). Carbothermic Reduction of Ferruginous Manganese Ore for Mn/Fe Beneficiation: Morphology Evolution and Separation Characteristic; *Minerals* 2017, 7, 167.
- Manganese. (2021, August 14). In Wikipedia
- Mariano, R. A. (2016). Mariano Measurement and Modelling of the Liberation and Distribution of Minerals in Comminuted Ores, *PhD Thesis University of Queensland Australia*, 1-265.
- Muriana, R.A., Muzenda, E., Abubakre, O.K., (2014). Carbothermic Reduction Kinetics of Ka’oje (Nigeria) Manganese ore. *Journal of Minerals and Materials Characterisation and Engineering*, 2, 92-99.
- Oyelola, A. O (2020). Upgrading a low grade Wasugu-Danko (Nigeria) Manganese Ore Using Gravity Separation Methods. *Indian Journal of Engineering*, 17 (4), 357-362.
- Rozenbaum, O., Machault, J., Le Trong, E., Tankeu, G. Y., Barbanson, L. (2015). Ore Fragmentation Modelling for the Evaluation of the Liberation Mesh Size. 13th SGA Biennial Meeting, *The Society for Geology Applied to Mineral Deposits*, France. 1447-1450.
- Sajjad, A., Yaseen, I., and Muhammad, F. (2019). A comprehensive phase, minero-chemical and microstructural investigation of low-grade manganese ore. *Material Research Express* (6) 115527. 1-8.
- Swapan , K. Haldar (2018). *Mineral Exploration: Principle and Applications*. Elsevier Science and Technology Book. 1-23
- Swapp, S. (2017). Scanning Electron Microscopy (SEM). *Geochemical and Instrumentation Analysis*
- Tangstad, M. (2013). *Handbook on Ferroalloy*. Elsevier Science and Technology Book 221-265.
- Welham, N. J. (2002). Activation of the carbothermic reduction of manganese ore. *Int. J. Miner Process*, 67 (2) 187–198.
- Wiegel, R. L. (1975). Liberation in Magnetic Iron Formation, *Trans. AIME*
- Wiegel, R. L. (2006). The Rationale Behind the Development of one Model Describing the Size Reduction/liberation of Ores. *Society of Mining Engineers*, 225-241.

- Wills', B. A. and Munn (2006). *Mineral Processing Technology*. Elsevier Science and Technology Book, 7, 60-80
- Wills, B., Napier-Munn, T., (2011). *Mineral Processing Technology: An Introduction to the Practical Aspect of Ores Treatment and Mineral Recovery*. Elsevier Science & Technology Books, Maryland Heights, MO, 59-80.
- Wills', B. A. (2015). *Wills' Mineral Processing Technology: An Introduction to the Practical Aspects of Ore Treatment and Mineral Recovery*, 8, 500- 512.
- Yaro, S. A., Hassan, B., Thomas, D. G. and Dodo, R. M., (2020). Characterisation of Wasagu Manganese Deposit; *Nigerian Journal of Engineering Faculty of Engineering Ahmadu Bello University Samaru - Zaria*, Nigeria, 27 (1), 12-50
- Zhang, J.; Subasinghe, N. (2013). Prediction of mineral liberation characteristics of comminuted particles of high-grade ores. *Miner. Eng.*, 49, 68–76.